ELECTRICAL STIMULATION TO PROMOTE SELECTIVE REINNERVATION OF DENERVATED LARYNGEAL MUSCLES

By

Yike Li

Dissertation
Submitted to the Faculty of the
Graduate School of Vanderbilt University
in partial fulfillment of the requirements
for the degree of

DOCTOR OF PHILOSOPHY
in
Hearing and Speech Sciences
December, 2016
Nashville, Tennessee

Approved:

David Zealear Ph.D.

Gaelyn Garrett M.D.

Bernard Rousseau Ph.D.

Daniel Ashmead Ph.D.

To my parents, who have been so supportive and dedicated to their son's education.

ACKNOWLEDGEMENTS

Firstly, I would like to express my sincere gratitude to my advisor Dr. Zealear for the continuous support of my Ph.D study and related research, for his patience, motivation, and immense knowledge. His guidance helped me in all the time of research and writing of this thesis.

Besides, I would like to thank the rest of my thesis committee: Dr. Garrett, Dr. Rousseau and Dr. Ashmead, for their insightful comments and encouragement, but also for the hard question which incented me to widen my research from various perspectives.

I thank Dr. Huang for the stimulating discussions we had, and for his instruction in surgical skills and animal care in the last seven years. I also thank Dr. Wu for her contribution to animal care and data collection throughout the study. Sincere gratitude is given to Amy Nunnally, Jamie Adcock and Phil Williams for their help with sterilized surgeries, without their contribution this dissertation would not be possible. The expertise and dedication of the staff of the Vanderbilt University Animal Care Facility was invaluable.

I am also very thankful to the experimental animals for their sacrifices, which contribute to improving the life quality of human beings. May their soul rest in peace.

Last but not the least, I would like to thank my parents for supporting me spiritually throughout my life in general. I would also thank my girlfriend, Cecilia, for being with me during days and nights of doing research and writing this dissertation.

TABLE OF CONTENTS

Page

LIST OF TABLES

LIST OF FIGURES

LIST OF ABBRIEVATIONS

(In order of appearance)

PCA ..... Posterior cricoarytenoid muscle

TA ..... Thyroarytenoid muscle

RGC ..... Reflex glottic closure

SLN ..... Superior laryngeal nerve

RLN ..... Recurrent laryngeal nerve

VFP ..... Vocal fold paralysis

ES ..... Electrical stimulation

EMG ..... Electromyography

DBS ..... Deep brain stimulation

IACUC ..... Institutional animal care and use committee

R/I ..... Rectified and integrated

UVFP ..... Unilateral vocal fold paralysis

BVFP ..... Bilateral vocal fold paralysis

BDNF ..... Brain-derived neurotrophic factor

IPG ..... Implantable pulse generator

NGA ..... Normalized glottic area

ANOVA ..... Analysis of variance

CO_2 ..... Carbon dioxide

CCD ..... Charge-coupled device

CHAPTER I

AN IMPLANTABLE ELECTRICAL INTERFACE FOR IN VIVO, CHRONIC STUDIES OF ELECTROMYOGRAPHY IN LARYNX FOLLOWING RECURRENT LARYNGEAL NERVE INJURY

INTRODUCTION

Normal laryngeal physiology requires complex interactions involving multiple components. These include both sensory and motor pathways for controlling coordinated muscle actions during voicing, airway protection and respiration. The posterior cricoarytenoid (PCA) muscle situated on the posterior larynx is the major abductor of the vocal fold. Contraction of this muscle enlarges the glottic area for inhalation. The thyroarytenoid (TA) muscle is the major adductor of the vocal fold to close the glottic airway during voicing and airway protection. Both abductor and adductor muscles are innervated by motor fibers in the recurrent laryngeal nerve (RLN). The abductor and adductor muscles are distinguished with respect to their motor unit composition [1, 2]**.** The PCA muscle exclusively contains inspiratory motor units that increase firing during hypercapnic or hypoxic conditions [3]. In stark contrast, the TA muscle and its synergists exclusively contain reflex glottic closure (RGC) motor units. They close the glottis reflexly upon activation of sensory receptors within the laryngeal mucosa. The afferent fibers of sensory receptors in the larynx are carried by the internal branch of the superior laryngeal nerve (SLN) [4].

Vocal fold paralysis (VFP) that results from injury to laryngeal motor axons in the RLN is a common, yet complicated clinical problem [1, 5, 6]. Damage to the RLN compromises both abducting and adducting functions as a consequence of laryngeal muscle denervation. In the majority of these patients, misdirected regeneration of neural

fibers in the RLN or collateral reinnervation from adjacent nerves (e.g. SLN, contralateral RLN) leads to a synkinetic larynx, where contraction of abductor and adductor antagonists produces ineffective, unsynchronized or even opposite movement of the vocal folds [1, 7, 8]. If the incomplete reinnervation or synkinesis is bilateral, the loss of vocal fold abduction on both sides results in a severe airway embarrassment that can be life threatening. There is currently no clinical intervention that will reliably prevent synkinesis or restore physiologic movement to the paralyzed vocal fold. Although evidence has indicated that electrical stimulation (ES) of the denervated PCA muscle with a low frequency may promote selective reinnervation by its original inspiratory motoneurons and reduce synkinetic vocal fold motion, the mechanism remains unknown [9].

Electromyography (EMG) plays an important role in exploring the mechanisms of selective reinnervation. In fact, laryngeal EMG has been applied in the studies on ES to provide important information regarding the innervation status of abductor and adductor muscles [2, 9]. However, recording of spontaneous and evoked EMG potentials was limited to the terminal session on each animal using invasive electrodes [9]. If a chronically implantable system was used, EMG recordings could be obtained repeatedly over time to provide chronological information regarding the reinnervation status of laryngeal muscles. The system would include nerve stimulation cuffs, muscle EMG electrodes, and an interface plug to make connections to external recording and stimulation equipment. Such an implantable system has been designed and used for canine laryngeal studies, but the interface plug was affixed to the skull and was susceptible to infection [2]. Possibly a better location for the interface plug would be on the skin, as demonstrated in studies of chronic EMG recording in rat hind limb muscles [10].

The purpose of the present study was to develop and test a simple, inexpensive, implantable system that could be used for repeated, temporary electrical connections between implanted components and external equipment for recording EMG from the canine larynx. This system could be used to record signals that reflect the innervation

status of target laryngeal muscles throughout the entire study with minimal risk of implant damage by the animal or infection.

MATERIALS AND METHODS

Description of the implant

This implantable EMG system consisted of two RLN bipolar nerve stimulus cuffs, two SLN bipolar nerve stimulus cuffs, two PCA EMG recording electrodes, two TA EMG recording electrodes, and an interface plug that permitted connection between each lead terminal and external equipment. Figure 1 shows a schematic of the components. A nerve stimulus cuff had two Teflon-coated stainless steel wires whose tips were deinsulated and attached to the interior surface of a silicon tube. Two 6-0 non-absorbable sutures were embedded into its wall for securing the cuff onto the nerve after installation. The recording electrodes were made of the same Teflon-coated stainless steel wires with hook-wire deinsulated tips. Attached to the TA recording electrode was a Dacron patch for additional electrode stabilization through suture fixation to the thyroid cartilage. All the Teflon-coated wires were coiled in order to provide spring-like motion of the leads during body movement to prevent breakage. A small metal female pin was attached at the other end of each electrode wire. During the implant surgery, all of the pins were inserted into the holes of a plug, which served as the interface for connection between all implanted electrodes and the external equipment.

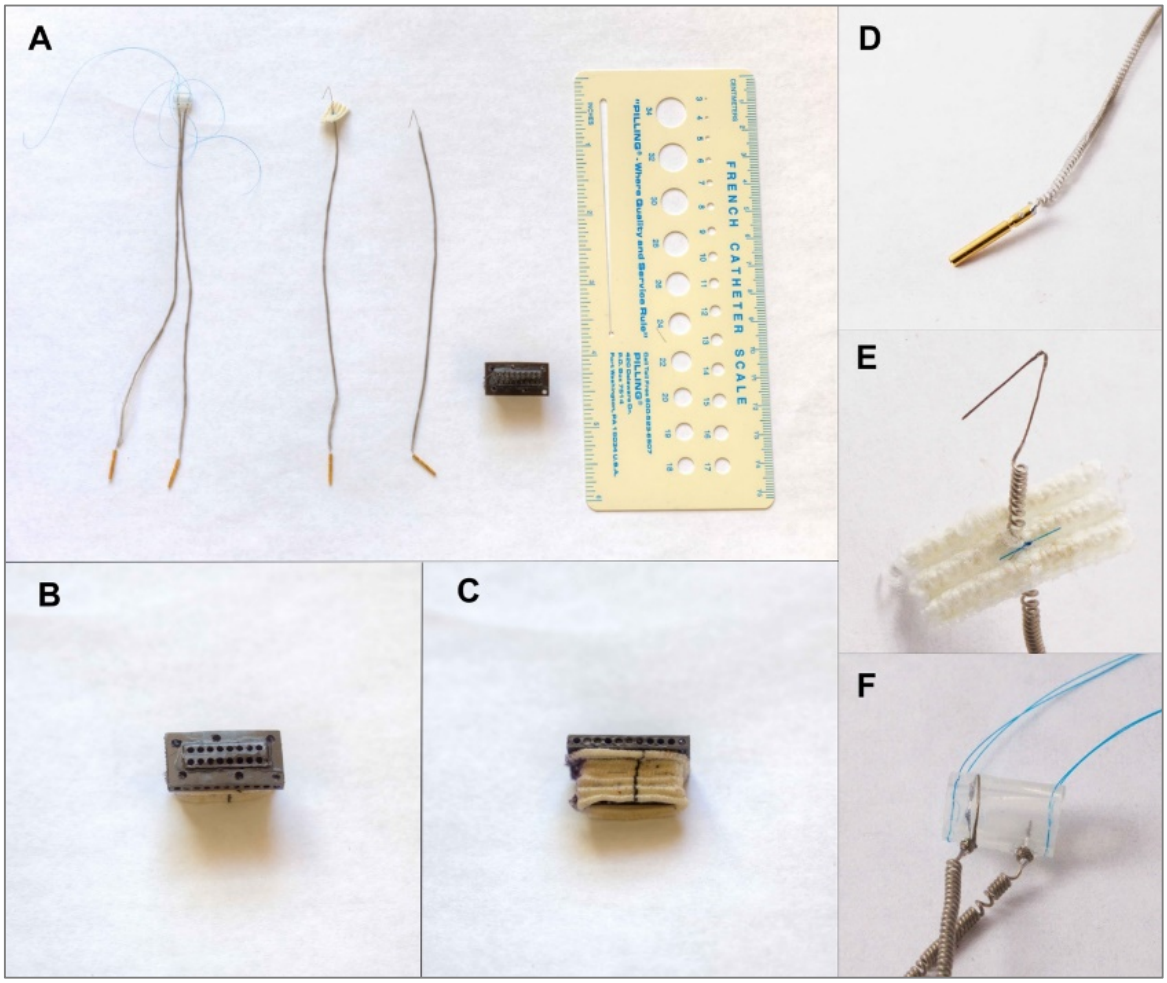

Figure 1. Stimulation and recording implant system. (A): From left to right is shown the stimulus cuff, the TA recording electrode, the PCA recording electrode, and the skin interface plug. Each Teflon-coated stainless steel lead wire was deinsulated 0.8 cm at the tip to form a hook-shape electrode for muscle recording (E). At the end of each wire was attached a female pin (D), which was inserted into a hole of the skin plug (B) during the surgery. The plug had Dacron attached on its sidewalls, which was designed to fix the plug in position by connective tissue anchorage to the mesh pores (C). Two 6-0 suture wires were embedded into the silicon tube of the bipolar nerve stimulus cuff (F).

An important application of this implantable EMG system was to obtain chronological EMG recordings from both the PCA and the TA muscle in animals undergoing bilateral RLN transection. In addition, a second implantable system was employed to chronically stimulate the PCA muscles to potentially effect the pattern of their subsequent reinnervation. This system consisted of two deep-brain-stimulation (DBS) electrodes

which were interfaced with an implantable pulse generator (IPG, EonC, St. Jude Medical Inc., St Paul, MN, USA). A detailed description of this implantable conditioning system will be presented in the second chapter of this dissertation. The PCA hook-wire recording electrode was inserted through the DBS electrode tip and fixed in position by Silicon gel (Figure 2, round inset).

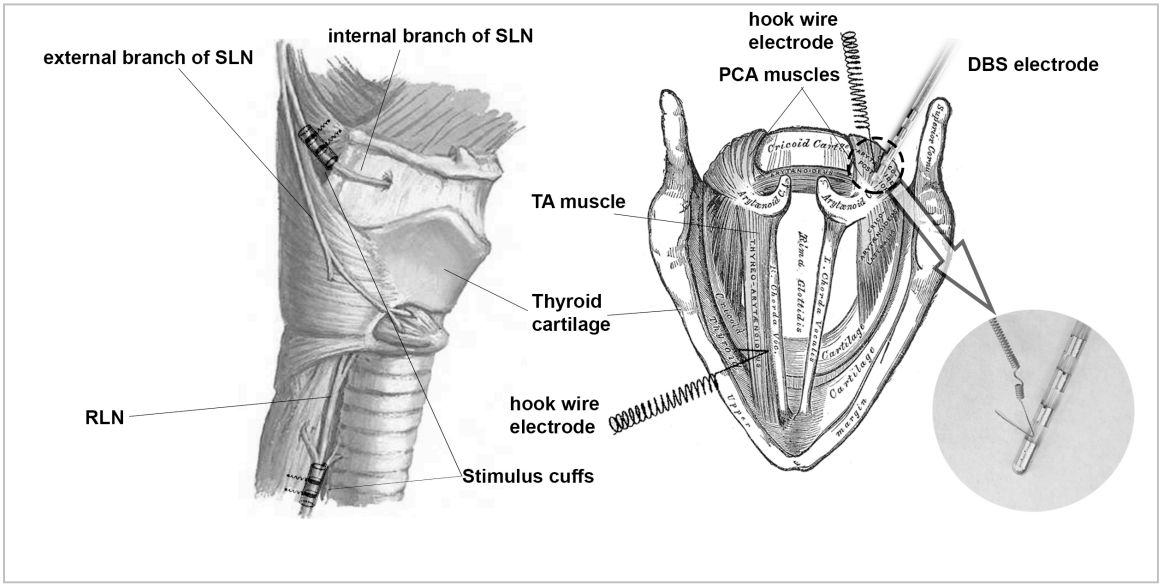

Figure 2. Schematic of implant in the larynx. Bipolar stimulus cuffs were implanted onto bilateral recurrent laryngeal nerves and internal branches of superior laryngeal nerves; hook wire recording electrodes were implanted in bilateral TA muscles and PCA muscles.

Implant surgery

This study was approved by the Institutional Animal Care and Use Committee (IACUC) of Vanderbilt University and conducted in accordance with the National Institutes of Health Guide for the Care and Use of Laboratory Animals. Eight adult canines weighing 20–25 kg were implanted with the device. They were mongrel hound strain obtained from Marshall farms (North Rose, NY, USA). Each dog was housed individually in an 87” x 42.5” cage with enrichment toys as well as normal food and water supply. These cages were located in an IACUC-approved animal housing facility with good ventilation and

12/12-hour light-dark cycle. Three of them (Dog #1 to #3) served as acute implant models in which their RLN nerves were left intact; the other five (Dog #4 to #8) were long-term animals with bilateral RLNs sectioned and anastomosed. Each animal was anesthetized with 2 mg to 4 mg/kg Telazol (Wyeth, Inc., Madison, WI) intravenously followed by 3% Isoflurane in oxygen through intubation. All procedures were performed under aseptic conditions. The animal was placed in a supine position and a midline neck incision was made from the thyroid notch to the manubrium. The trachea was dissected free from the esophagus, and the inferior border of the cricoid cartilage was exposed. The stimulus cuffs were positioned onto the SLNs and RLNs bilaterally and the lips of each cuff sutured for closure. A cartilage window was made by a biopsy punch at the anterior surface of the thyroid cartilage on each side and both TA muscles were exposed. The EMG recording electrodes were inserted into the TA muscles using a 23-gauge needle. Sutures were made between the electrode Dacron patch and cartilage. The DBS electrode along with the hook-wire EMG recording electrode was placed underneath the PCA muscle on each side (Figure 2). After endoscopic confirmation that stimulation produced vocal fold abduction for each channel, the DBS electrodes were anchored to the cricoid cartilage by 4-0 silk. All the wire leads of the EMG system were connected to the interface plug and pinched into holes with an insertion tool fashioned from a hemostat. Bone cement (Zimmer, Warsaw, IN) was used to seal the inferior side of the plug to insulate lead-pin junctions. The plug was placed at the rostral end of the midline incision through the skin and was sutured to subcutaneous tissues and skin. The two DBS leads were connected to the IPG which was positioned underneath the trapezius muscle on the left side of the neck. For the long-term animals, a second surgery was performed to transect and anastomose the RLNs 9 to 16 days after the first implant surgery. Baseline recordings could be obtained between the two surgeries while the nerves were intact. Each animal was closely monitored postoperatively until full recovery from the surgery. Buprenorphine was given twice a day for up to 3 days postoperatively to minimize any discomfort or pain. Tranquilizers or antibiotics were used when necessary. To allow normal wound healing and stabilization of implanted devices, each animal was restricted from exercise for a period of 10 days.

EMG recording during physiology session

Following implantation, each animal was brought to the laboratory every 2-3 days in the first week and then once a week thereafter. The animal was anesthetized with Telazol (initial loading dose 2–4 mg/kg i.v., then maintained with 0.4 mg/kg per hour) and maintained in a moderate plane of anesthesia in a supine position. A zero degree endoscope (Karl Storz, Germany) with an attached Sony CCD (Sony Corp., Tokyo, Japan) video camera was inserted through a laryngoscope to visualize vocal fold motion at the level of the glottis. An external plug similar to the interface plug but smaller and integrated with male pins connected the muscle electrode leads to external preamplifiers for EMG recording (Grass P5 Preamplifiers, Grass Products, RI, USA, Figure 3). Individual male pins were used to connect the nerve stimulation electrodes to a pulse generator (Grass S88 stimulator, Grass Products, RI, USA). The outputs from the preamplifiers were connected to two sets of recording equipment: The first set consisted of two oscilloscopes (Digital Recording Oscilloscope 1604 & Fast Recording Scope 7200, Gould Electronics, USA) that were configured differently to record and analyze peak-to-peak values (DRO 1604) and rectified and integrated areas (FRS 7200) of EMG signals; The second set was PowerLab 16/35 (ADInstruments, Inc, CO, USA) that served as analog-to-digital hardware, it was connected to a laptop where EMG data was displayed and stored for off-line analysis.

First, to start data collection, evoked EMG responses were recorded from TA and PCA muscles following RLN stimulation. Since the RLN contains nerve fibers of both inspiratory and RGC motor units, stimulation of RLN resulted in firing of both types of units. Therefore, the evoked EMG response recorded from the PCA and TA muscles gave a good index of the overall magnitude of their innervation or reinnervation, irrespective of motor unit type. Evoked EMG motor unit activity was rectified and integrated over a 20-ms window.

Second, the internal branch of the superior laryngeal nerve was stimulated. Sensory-elicited motor unit activity was recorded from the PCA and TA muscles. Recorded RGC

unit activity was quantified by rectification and integration over a 20-ms window, positioned in time to capture the entire RGC waveform. As only the RGC units were recruited by stimulation of the SLN, the recorded muscle activity gave an estimate of incorrect reinnervation of the PCA muscle and correct reinnervation of the TA muscle.

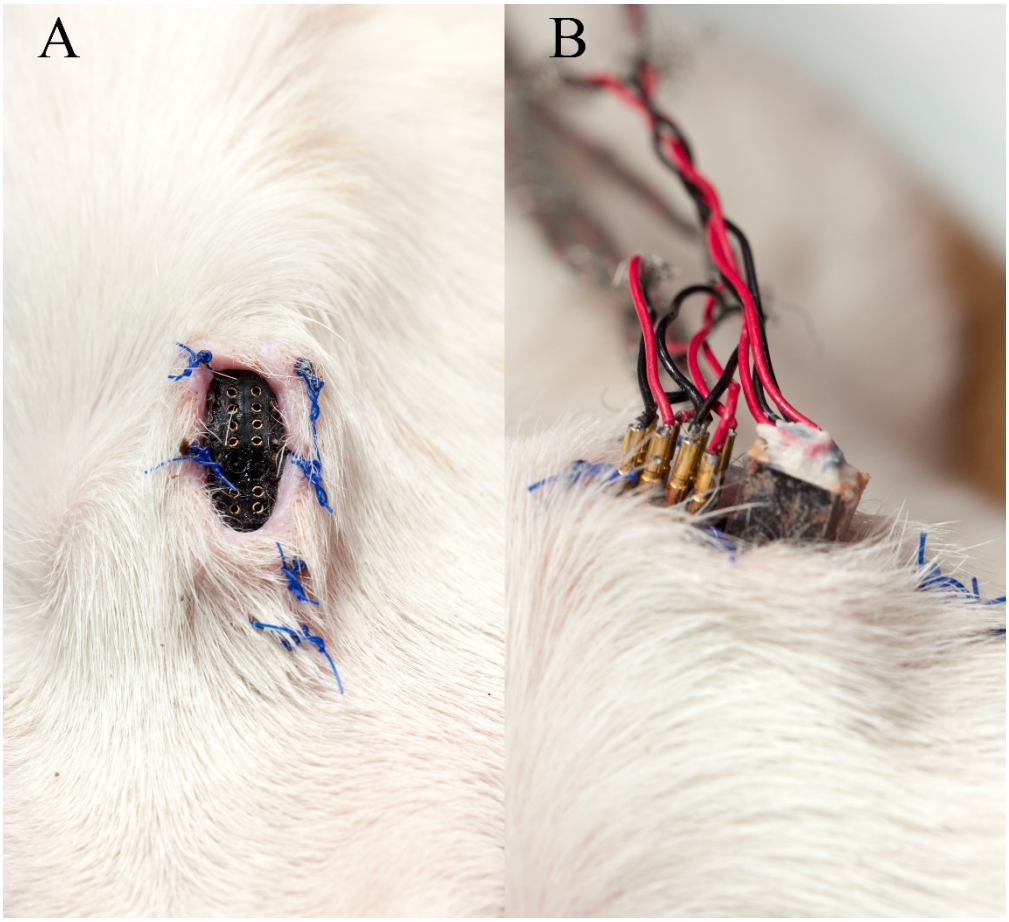

Figure 3. The interface plug on the skin of the anterior neck (A) and connections that were established for nerve stimulation and EMG recording in the experiment (B). Dummy male pins were put inserted into the female pins of the plug to keep them free of debris between recording sessions.

Finally, spontaneous EMG activity was recorded from PCA and TA muscles when respiratory drive was maximized by administration of CO2 mixed with room air. Exposure was limited to 1 minute during which time maximum inspiratory motor unit recruitment occurred. Recordings were amplified, rectified, and integrated over an 8-second time interval. Normally, inspiratory motor units were involved in abducting the

vocal cord at maximal inspiratory effort; such spontaneous EMG activity provided a good estimate of the magnitude of appropriate PCA muscle reinnervation by its original inspiratory motoneurons. Likewise, the inspiratory EMG activity recorded from the TA gave an index of the incorrect or synkinetic reinnervation of this muscle.

RESULTS

Device compatibility

The duration of the study ranged from 7 to 10 weeks (9±1.7, Mean±SD) for the short term animals, and from 6 to 41 weeks (32±14) for the long term animals. One long-term animal (Dog #6) was removed from the study at 6 weeks because of failure of the IPG, his EMG recording system remained intact and functional. Seven of the eight canines tolerated the implants well throughout the study. Only the first short term implant (Dog #1) showed signs of infection by the end of the study, as demonstrated by skin irritation and purulent discharge around the interface plug. For the rest of the animals, the skin around the interface plug appeared healthy and the sutures securing the plug remained intact (Figure 3A).

Post-mortem examination revealed that the inferior part of the interface plug was typically encapsulated by connective tissues. Such encapsulation not only fixed the skin plug in position, but also helped stop bacteria tracking down leads and causing infection in deeper tissues. Similar encapsulation occurred around implanted leads and electrodes but it did not interfere with the function of the system.

No sign of degradation or erosion was evident in any wire lead, electrode, or the plug. The nerve stimulus cuffs remained in position and functional in most cases except for one, in which a suture on the cuff became loose and part of the nerve slipped out of the slit. Generally, the size of the cuff was large enough to prevent neuropraxia from

postoperative edema, yet small enough to permit nerve excitation. All the lead wires remained intact and coiled. All recording electrodes were kept in position and remained functional.

Nerve trauma was seen in one acute implant case (Dog #3), as evidenced by the lack of evoked response from both PCA and TA muscles during RLN stimulation on the same side. This was probably due to iatrogenic injury during dissection of the RLN, as the cuffs and electrodes were found to be anatomically in position and intact during autopsy. EMG potentials could not be recorded from a PCA muscle in one case, and autopsy showed the hook-wire recording electrode had been inserted into the perichondrium of the cricoid cartilage.

Although these problems were encountered in short-term implant animals, they were all resolved in long-term animals after gaining sufficient experience and skill in postoperative care and surgical technique.

EMG recordings

EMG signals were successfully recorded from the PCA and TA muscles in almost all animals. The shape and the amplitude of the potentials were comparable to what we recorded previously [2]. Stimulus artifact was minimal and did not impact the evoked muscle signal.

In the normally innervated larynx, the PCA or TA response evoked by stimulation of the RLN (Figure 4A, large peak) had a shorter latency than the TA response evoked by stimulation of the SLN (Figure 4B, largest peak(b)) because the former involved a monosynaptic pathway while the latter involved a reflex polysynaptic pathway. Further, the direct response due to activation of motor fibers in the RLN was distinguished in the consistency of its EMG waveform across stimulus trials in contrast to the indirect variable response of RGC motor units recruited by SLN stimulation. After the occurrence of stimulus artifacts (arrows), laryngeal muscle potentials appeared. The potential (a)

immediately following the stimulus artifact in Figure 4B was a direct response from the cricothyroid muscle, since this muscle was also innervated by the SLN. The cricothyroid potential was recorded by the TA electrode since this muscle was located near the TA muscle. Previous studies have shown that the cricothyroid component of the SLN response can be selectively abolished by sectioning the external branch of the SLN (Zealear, unpublished observations).

Spontaneous EMG signal from the PCA muscles manifested phasic inspiratory discharges followed by minimal expiratory activity during each respiratory cycle at rest. (Figure 4C) Upon CO2 delivery through the mouth, an increase in muscle activity was typically observed within 20 seconds after the start of a CO2 trial, indicating contraction of the abductor muscle to open the vocal fold during hypercapnic breathing. (Figure 4D). The amplitude of an individual evoked EMG signal was measured in the form of a rectified/integrated (R/I) area over a 20-ms window. Table 1 summarizes the amplitude of all EMG signals recorded when the nerves were intact. A typical EMG signal recorded from the PCA muscle in response to the RLN stimulation ranged from 8 to 14 μV*s which was marginally smaller than the response of TA muscle by RLN stimulation (15-23 μV*s). In contrast, only the TA muscle showed response to the SLN stimulation because the RGC units exclusively innervate adductor muscles. The amplitude of TA responses ranged from 7 to 13 μV*s, averaging 10.5 μV*s, while the PCA amplitude following SLN stimulation did not differ from the background noise level. During CO2 breathing, the PCA muscle was exclusively activated to abduct the vocal folds and enlarge the glottis. This was accompanied by a large increase in EMG activity over baseline levels, averaging 0.8 mV*s for an 8-second rectification-integration period. This was significantly larger than the EMG noise level of the TA muscle, which averaged only 0.2mV*s.

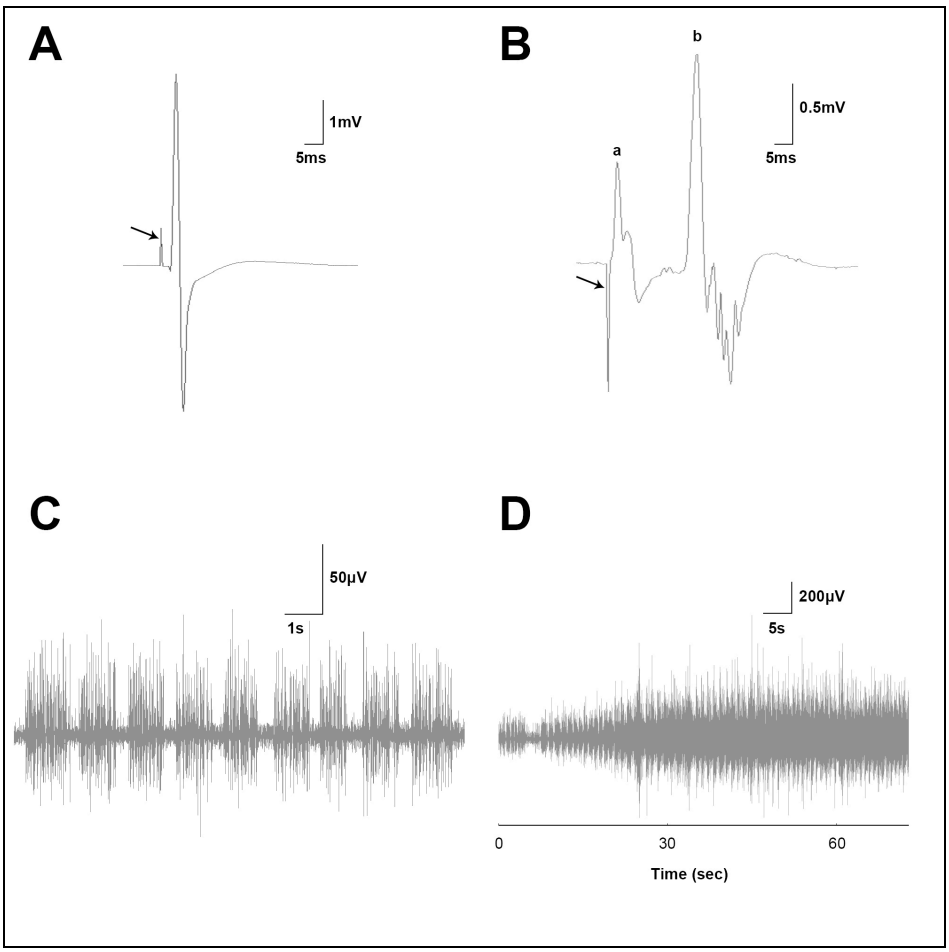

Figure 4. EMG Recordings from laryngeal muscles. A: evoked electromyography (EEMG) from PCA muscle following RLN stimulation. B: response of TA muscle RGC motor units activated polysynaptically via SLN stimulation. C: normal spontaneous inspiratory activity recorded from PCA muscles. D. EMG activity from PCA muscle throughout the course of CO2/air delivery.

Canine	RLN		SLN		CO2	
	PCA	TA	PCA	TA	PCA	TA
#1	14.7±3.1	14.7±3.0	0.9±0.3	7.9±2.0	0.9±0.2	0.2±0.1
#2	10.6±1.8	19.4±5.0	1.8±0.7	7.6±2.0	0.6±0.1	0.2±0.1
#3	N/A	23.3±2.9	3.3±0.5	13.0±3.1	1.0±0.2	0.3±0.1
#4	8.4±2.6	14.0±5.4	1.9±0.6	9.7±3.6	0.7±0.1	0.2±0.1
#5	13.8±1.6	18.9±2.0	1.8±0.6	10.0±2.0	0.9±0.3	0.1±0.1
#6	11.0±2.7	17.6±3.7	1.2±0.5	13.4±3.0	0.7±0.1	0.1±0.1
#7	9.6±1.8	16.4±2.5	1.5±0.3	13.0±1.9	0.6±0.2	0.2±0.1
#8	11.4±4.9	16.8±2.2	2.0±0.4	9.4±1.1	0.9±0.2	0.2±0.1
Mean	11.5±3.4	17.7±4.3	1.7±0.8	10.4±3.1	0.8±0.2	0.2±0.1

Table 1. Amplitude of evoked and spontaneous EMG responses recorded from laryngeal muscles when RLNs were intact. All values were shown in the form of mean ± standard deviation. Abbreviation: RLN-Recurrent Laryngeal Nerve; SLN-Superior Laryngeal Nerve; PCA- Posterior cricoarytenoid muscle; TA- Thyroarytenoid muscle.

Following RLN nerve section and repair, the overall level of PCA and TA muscle reinnervation could be quantified by the amplitude of their EMG potentials evoked by RLN stimulation (Figure 5). In 4 chronic animals, substantial EMG responses were recorded in both PCA and TA muscles preoperatively. Following RLN transection, responses from both muscles were at noise level during the first two months. The EMG signal typically reappeared in both PCA and TA muscles after 2 months and reached a plateau by 5-6 months. All four TA muscles regained substantial magnitude of reinnervation by the end of the study, as their EMG responses was comparable to their preoperative baseline levels (14-21μV*s). Similarly, the PCA muscles in two animals (#4 and #8) had considerable overall reinnervation while the other two (#5 and #7) had substantially less.

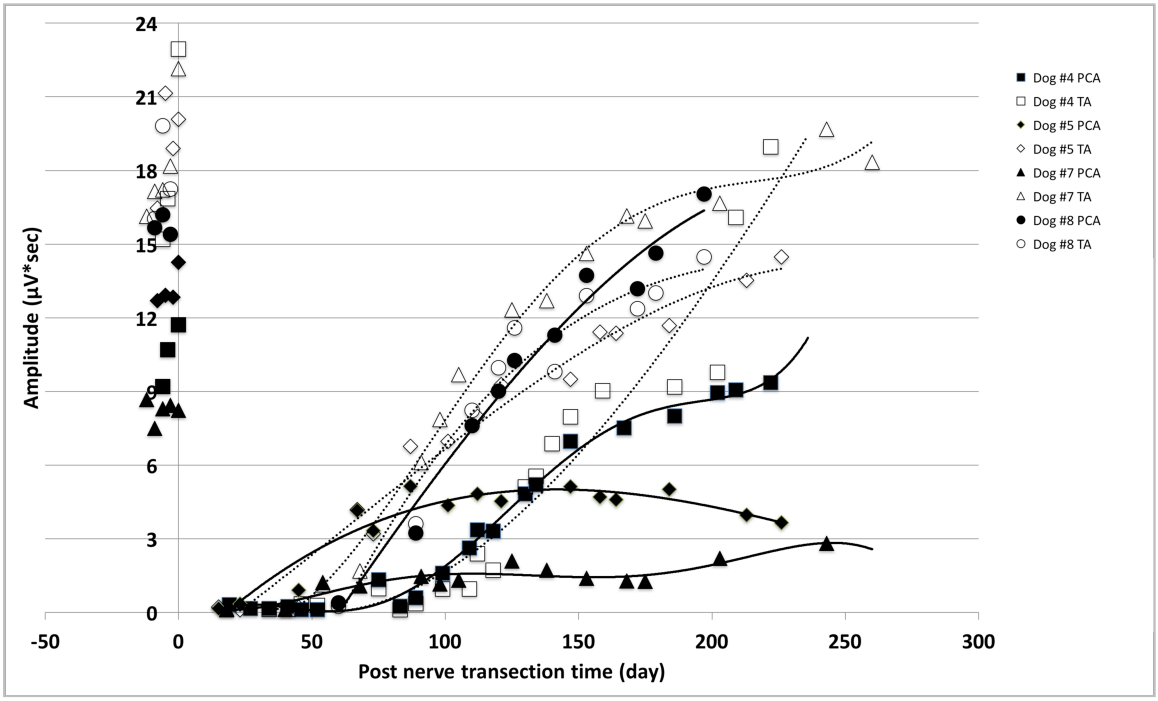

Figure 5. Chronological recordings of potentials evoked by RLN stimulation from four long-term nerve-sectioned animals.

The level of incorrect reinnervation of the PCA muscle and correct reinnervation of TA muscles by RGC motor units can be indexed by the relative responses evoked by SLN stimulation. Figure 6 shows chronological recordings of potentials evoked by SLN stimulation (i.e. the RGC response) from 4 long-term nerve-sectioned animals. Before nerve section (time 0), RGC responses were only recorded from the TA muscles. The PCA amplitudes were at noise level. Thus RGC motor units exclusively comprised the TA muscle. Following nerve section, the RGC response typically reappeared in the TA muscles in about 2 months, and reached a plateau by 5-6 months. In three animals (i.e. Dog #4, #5 and #7), reinnervation of the PCA muscles by foreign RGC motoneurons was inhibited. In contrast, the fourth animal (i.e. Dog #8) showed synkinetic reinnervation of the PCA muscle.

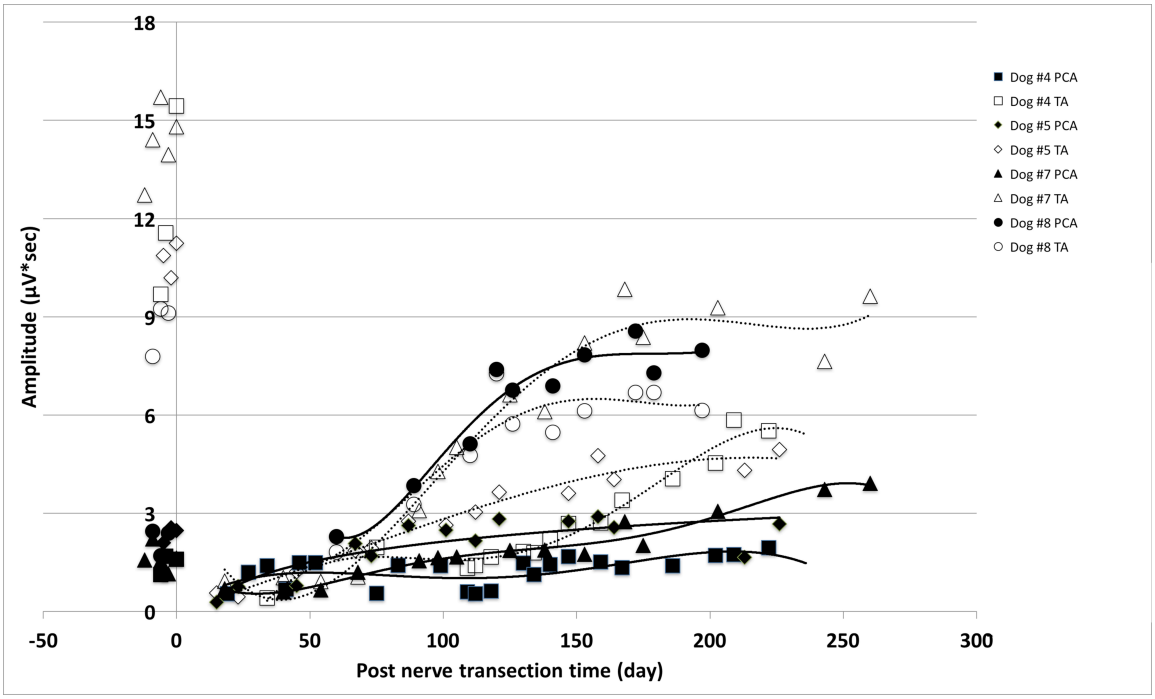

Figure 6. Chronological recordings of potentials evoked by SLN stimulation (i.e. the RGC response) from four long-term nerve-sectioned animals.

DISCUSSION

This chapter presented a chronic EMG implant method and system that was simple and capable of obtaining stable EMG recordings from both abductor and adductor muscles in the canine's larynx for up to 41 weeks. Several advantages were observed: The design of the skin interface plug was uncomplicated and compact, but sufficient for its purpose. Temporary electrical connection to external equipment could be easily established by inserting wire containing male pins into the female pins of the skin plug. The Dacron attached on the sidewalls helped to fix the plug in position by connective tissue anchorage to the mesh pores. The small size of the plug and its location on the anterior neck prevented device breakage by an animal's activity while not causing discomfort to the animal. Use of hook wire tips increased the stability of the EMG electrodes in the muscle. Coiling lead wires provided additional flexibility and prevented leads from breaking during bending movement. The procedure of tunneling the wires subcutaneously added stability to the implant as the fascia bonded well to the wires' insulation. Risk of infection was minimized by several procedures: (1) After insertion of the female pins into the holes of the skin plug, the subcutaneous surface of the plug was sealed by bone cement, which helped to keep bacteria tracking down from the external surface; (2) The surgical wound was flushed with gentamycin and postoperative antibiotics were also given orally to all the animals for at least three days; (3) The skin plug was cleaned daily with Nolvasan solution (Fort Dodge, Overland Park, KS), removing any debris that could have caused instability of electrical connection. (4) In addition, dummy male pins were positioned into the holes of the skin plug at all times except during the EMG recording sessions. This maneuver kept the female pins free of debris, which allowed competent connections to be made by the interface cable. Trauma and edema were minimized as well. The dogs were able to perform behavioral tasks within a few days of the surgery. Necropsy showed adequate encapsulation of all the implants. Dissection along the course of the wires showed no evidence of inflammation. All of these advantages made this implant system more preferable to the skull mounting plug, which was prone to infection.

Several problems were encountered in this study. First, infection was observed in the first implant. It was probably due to inadequate cleaning of the skin plug, since the infection started from the skin in about two months after the implant surgery and necropsy showed no sign of infection in deeper tissues. The plug was cleaned 2-3 times per week in this animal. In subsequent animals the plugs were cleaned daily and there was no sign of infection throughout the duration of the study in these animals. Second, iatrogenic injury was observed in another acute implant case, in which RLN was injured by extensive dissection. As operative skill and postoperative care improved, no infection or iatrogenic injury was encountered in the long-term animals.

The positions of the recording electrodes for both the PCA and the TA muscles were confirmed by post-mortem microdissection of the larynx. There was no sign of any electrode migration in any long term animal. Thus the absence of an EMG response from a muscle in these long term animals likely resulted from little, if any, reinnervation of the muscle, instead of electrode migration.

On the whole, this implantable system was simple, economical and functional, which made it a reliable platform for EMG measurement in any research application where chronological recordings need to be made over long periods of time. It could be applied to other neuromuscular studies where neural stimulation and/or chronic EMG recording are required, such as investigations of swallowing and facial paralysis. In this regard, the technology as described is being used to study tongue plasticity through hypoglossal nerve stimulation in the awake chronically implanted aging rat **[10]**. It should also be mentioned that this implantable system could be combined with remote recording technology (e.g. telemetry) to provide a means for EMG recording in freely moving animals. As such, it could be viewed as a platform technology for long-term intramuscular recording. We have demonstrated the functionality and reliability of the system in electrophysiological studies of laryngeal muscles in both short term and long

term animals for up to 41 weeks. Clinical experience with implantation indicated minimal surgical difficulty and postoperative complications. Future research will include evaluation of this system in an animal model for examining the effect of electrical stimulation on selective reinnervation of paralyzed facial muscles.

CONCLUSION

A simple, inexpensive implantable system was developed for long-term EMG recordings from the canine's larynx. Use of this device could record reliable EMG signals that reflected the innervation status of the target laryngeal muscles throughout the entire study with minimal risk of device breakage, trauma or infection.

CHAPTER II

ELECTROSTIMULATION OF DENERVATED LARYNGEAL MUSCLES TO PROMOTE SELECTIVE REINNERVATION

INTRODUCTION

The term vocal fold paralysis conjures the image of a motionless larynx. The symptomatology of VFP depends upon whether the damage to the nerve is unilateral or bilateral. Patients with long-standing unilateral vocal fold paralysis (UVFP) typically present with a fairly sudden onset of breathy, weak, low-pitched dysphonia. Some of these patients may report shortness of breath or a feeling of running out of air, due to the glottal incompetence during speech. UVFP may also be associated with dysphagia or aspiration. As a result, vocal fold injection or thyroplasty may be provided to patients with UVFP to improve vocal quality by restoring glottal competence and to improve swallowing function [11-13]. Compared to UVFP, where normal ventilation can be relatively spared with only one vocal fold paralyzed, the classical presentation of patients with bilateral vocal fold paralysis (BVFP) is reduction of glottal area. Airway obstruction with distressing, persistent, high-pitched stridor is usually severe enough to warrant tracheotomy. In many patients, clinical intervention is required in the form of an emergent tracheotomy followed by a partial resection of the vocal fold to enlarge the airway (e.g cordotomy, arytenoidectomy) and return breathing through the mouth. Unfortunately, this procedure sacrifices voice and compromises the ability to swallow without aspiration [6].

Neither of these airway enlargement procedures can restore both major functions of the larynx—enlargement of the airway for respiration and reduction for vocalization. For either type of VFP, especially BVFP, an ideal treatment approach would be to allow nerve regeneration following injury to restore natural reinnervation of muscles and avoid

synkinetic paralysis altogether. Since Horsley's original report of successful restoration of vocal fold mobility after RLN anastomosis [14], some investigators have attempted to reinnervate the paralyzed larynx using a variety of approaches in animal experiments and limited clinical trials [15-18]. However, results of procedures by RLN anastomosis have not been favorable in terms of restoring the spontaneous and/or voluntary motility of the larynx [19]. Poor functional outcomes following repair of peripheral nerve lesions can be attributed to two main factors: (1) decreased magnitude of reinnervation to the target organ in face of tissue atrophy, and more importantly (2) misdirected regenerating axons into the wrong distal pathways and inappropriate target reinnervation [20, 21].

Electrical stimulation (ES) has emerged as a potential therapeutic measure following peripheral nerve injury to prevent muscle atrophy and enhance nerve regeneration. It has been shown that ES to the denervated muscle prevents loss of muscle mass and strength and may improve function in hind limbs [22-25], larynx [26, 27], face [25] and hands [28]. Recent evidence showed that ES to the muscle significantly reduced the expression of muscle-specific ubiquitin ligase - muscle RING finger 1 (MuRF-1), which is normally overexpressed in atrophied muscles [29]. In addition, ES applied to the nerve may also promote functional recovery of the muscle after denervation [2, 30-33]. Al-Majed et.al. demonstrated that ES to the nerve accelerates axon outgrowth by mediating the expression of brain-derived neurotrophic factor (BDNF) and its specific receptor trkB at the level of neuron cell body [34]. The up-regulation of both BDNF and trkB is crucially involved in the up-regulation of regeneration-associated genes such as Tα1-tubulin and growth-associated protein 43 (GAP-43). These genes are also implicated in the subsequent acceleration of axonal elongation [35]. All this evidence indicated that ES contributed to functional recovery of the denervated muscles by accelerating axon regeneration and reinnervation of muscle before significant atrophy had occurred [20].

On the other hand, the effect of ES on the specificity of reinnervation is less well understood. In the rat hind limb, Brushart et. al. demonstrated that motoneurons preferentially regenerate down the motor branch at a motor-sensory bifurcation pathway [36]. This process is believed to be triggered by Schwann cell neurotrophins and directed

by motoneuron cell bodies. Specifically, ES applied briefly to motoneurons was found to accelerate the speed and accuracy of regeneration down a motor pathway [20, 37]. However, preferential motoneuron regeneration down one muscle pathway versus another does not appear to occur naturally following lesion of a common nerve composed of mixed efferents. Indeed, inappropriate muscle reinnervation is prominent following injury to such nerves as the facial or recurrent laryngeal nerves. Regarding the latter, synkinesis could be avoided only by stimulating the muscle or its reconnecting motoneurons as shown by Zealear et. al. [2]. In this study, there was quantitative evidence that low frequency stimulation of the PCA muscle repressed reconnection by foreign RGC motoneurons and promoted reinnervation by native inspiratory motoneurons. The hypothesis for the mechanism through which ES enhances the specificity of reinnervation was postulated: ES modulates not only contractile protein synthesis and muscle fiber properties, but also receptivity of the endplate for a particular motoneuron type.

Although the mechanism for ES underlying selective reinnervation is not known, these previous findings should encourage further investigations of ES to enhance selective reinnervation by stimulating the PCA muscle during a critical period of reinnervation following RLN injury, which may lead to a preferable and natural approach to treatment of synkinetic VFP. Further, the application of ES to other motor systems could provide benefit if synkinetic paralysis is commonly manifested. For example, Bell's palsy may also be treated with ES once the mechanism underlying selective reinnervation is fully discovered in the canine laryngeal model.

A particular ES paradigm can be defined through its frequency, pulse duration, duty cycle, amplitude, ramp time, pulse waveform, train duration, train frequency, etc. [38]. If ES of the muscle can promote selective reinnervation by its original motoneurons, it will be interesting to find out whether this effect varies when using different stimulus paradigms. To design a study to answer this question, we'd like to focus on those parameters that are most likely to have an impact on the pattern of reinnervation.

To find out what parameters are critical, it is important to understand the properties of motoneurons and muscle fibers, as well as their relationship. As a matter of fact, it has long been realized that there is a fundamental relationship between an α-motoneuron and the muscle fibers it innervates, for which the term motor unit was coined [39]. A motor unit is made up of a motoneuron and the skeletal muscle fibers innervated by that motoneuron's axonal terminals [40]. Motor units can be categorized based upon their response characteristics, or more specifically, their contraction speeds. Generally, there are two types of motor units based on this classification: slow and fast. The motoneurons of slow motor units exhibit tonic activity at low firing frequencies, and slow muscle contraction speed with low force. In contrast, the motoneurons of fast motor units typically exhibit phasic activity at high firing rates and fast muscle contraction speed with high force [41]. The most distinctive feature of these types of motoneurons is their firing frequencies.

The pioneering study of Buller et.al. was the first to establish that muscle fiber physiological properties were correlated with those of their motoneurons [42]. Since then, many studies have been done to investigate the role of motor innervation in maintaining or changing muscle properties using various methods such as denervation, cross-reinnervation and ES. It is well established that muscle physiological properties and chemistry are under the control of the electrical impulse pattern mediated by its nerve supply [43-49]. Moreover, ES of denervated muscle at frequencies that mimic normal slow-twitch or fast-twitch motor unit activities result in transformation of the muscle to each type, respectively [43, 45, 48-50]. In sum, ES takes advantage of a muscle's inherent plasticity by modulating the contractile protein synthesis and muscle fiber properties. With this knowledge, it has been postulated that the receptivity of the endplate for a particular motoneuron type can also be modulated by varying the pattern of ES conditioning of the muscle [2]. That is, it is hypothesized that the induced activity affects the pattern of reinnervation as well as the muscle's contractile properties in a way largely determined by the frequency of stimulation [45, 46].

As mentioned earlier, the abductor (PCA) and adductor (TA) muscles are distinguished with respect to their motor unit composition. The PCA muscle exclusively contains inspiratory motor units which typically have slow firing rates and increase firing during hypercapnic or hypoxic conditions [3]. In contrast, the TA muscle and its synergists exclusively contain fast-firing motor units and close the glottis reflexively by activation of sensory receptors within the laryngeal mucosa [21]. According to the hypothesis, the type of neurons that reconnect with the PCA muscle may depend upon the type of activity presented during the conditioning period. The goal of this study was to determine if low frequency stimulation, characteristic of slow motoneurons such as PCA inspiratory neurons, would lead to a more appropriate PCA muscle reinnervation and better glottic airway compared to high frequency stimulation. The long term EMG recording technique described in the first chapter was used to accomplish this aim.

MATERIALS AND METHODS

Experimental design and stimulus paradigm

This study was performed in accordance with the PHS Policy on Humane Care and Use of Laboratory Animals, the NIH Guide for the Care and Use of Laboratory Animals, and the Animal Welfare Act (7 U.S.C. et seq.). The animal use protocol was approved by the Institutional Animal Care and Use Committee of Vanderbilt University. Eleven canines (body weight 21-26 kg) were entered into the study and randomly assigned to four groups to assess the effect of different stimulus paradigms on reinnervation quality and degree of functional recovery: 1) non-stimulated control 2) 10Hz 3) 20Hz 4) 40Hz train (Table 2). Stimuli were applied to the PCA muscles during the denervation/regeneration period of 90 days using a totally implantable system. In the stimulation groups, the left PCA was stimulated continuously and the right PCA once a week in all except one animal (#940). Only a small number of animals could be studied because of the long duration required to

assess reinnervation and functional outcome. Preoperative testing of animals with intact RLNs was performed to obtain normal data for comparison with postoperative data during endoscopy and treadmill testing. In addition, a separate control group with intact RLNs was added for comparison of PCA and TA EMG data following nerve section and reinnervation.

Grouping (Stimulus frequency)		**Non-stimulation**		**10Hz**			**20Hz**		**40Hz**			
Animal number		510	858	575	753	940	824	874	345	688	509	36
Study duration (months)		10	8	12	12	9	10	7	20	10	14	8
Stimulus paradigm applied to the PCA muscle	Continuous	No stimulation until respiratory impairment		L	L	R	L	L	L	L	L	L
	Two hours, once per week			R	R	L	R	R	R	R	R	R

Table 2. Animal Groupings and stimulus paradigms. Pulse trains were delivered to animals' PCA muscles in different frequencies with 4-sec on/ 4-sec off duty cycle; L-Left; R-Right

Implant surgery

Each animal was anesthetized with 2–4 mg/kg Telazol (Wyeth, Inc., Madison, WI) intravenously followed by 3% Isofluorane in oxygen through intubation. All procedures were performed under aseptic conditions. The animal was placed in a supine position and a midline neck incision made from the thyroid notch to the manubrium. The trachea was dissected free from the esophagus, and the inferior border of the cricoid cartilage was exposed. On each side, a submuscular pocket was created between the PCA muscle and the underlying cricoid cartilage using a periosteal elevator. A deep brain stimulation (DBS) electrode was inserted 14.5 mm into each pocket halfway between the point of RLN entry and the median raphe, with a trajectory parallel to the midline (Figure 7, right PCA electrode inserted). After endoscopic confirmation that stimulation produced vocal fold abduction for each channel, the electrodes were anchored to the cricoid cartilage by

4-0 silk. The channels were numbered 1 to 4 on the left side and 5 to 8 on the right side from tip to base of each electrode. The electrode leads were interfaced with the implantable pulse generator (IPG) which was positioned in a submuscular pocket beneath the trapezius muscle within another lateral incision. After implantation, IPG stimulus parameters could be changed transcutaneously with an external programmer through a radio frequency link. The RLNs were transected 5 cm from the cricoid bilaterally and anastomosed using 6-0 Prolene suture (Ethicon Inc., Somerville, NJ). The neck incision was closed and antibiotics were administered for 4 days perorally. In four of the eleven animals, the EMG system described in Chapter 1 was also implanted to obtain chronological data regarding the selective reinnervation status in these animals. Nerve transection was delayed for approximately 10 days and performed in a second surgery so that normative EMG data could be obtained in each animal. Because of the risk of ventilatory compromise and aspiration following nerve section, the animals were periodically monitored and given soft food by hand for 7 days postoperatively. Chest x-ray and videofluoroscopy with barium swallow were performed preoperatively and at regular postoperative intervals [GE-OEC 9900 Elite Mobile X-ray C-arm system (General Electric Healthcare, Inc, Piscataway, NY)].

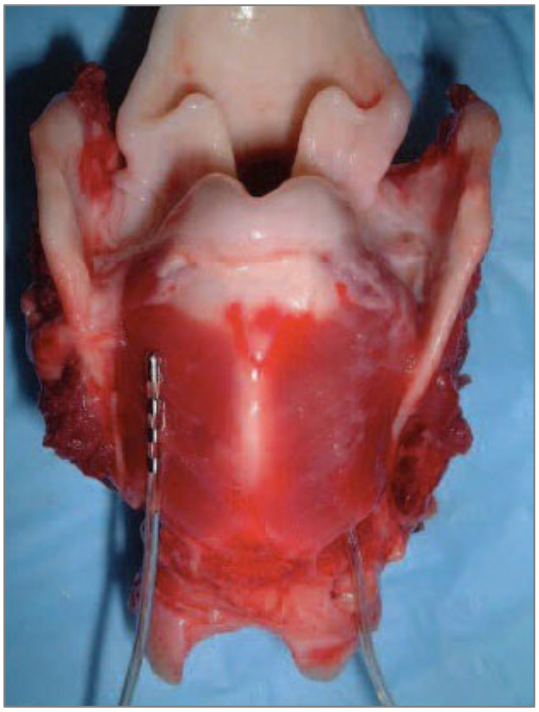

Figure 7. Posterior view of the canine larynx display the deep brain stimulation electrode inserted into the submuscular pocket of the right PCA muscle.

Endoscopic sessions

Endoscopic sessions were conducted on each animal every 2 weeks during the period of denervation and the dynamic phase of reinnervation (first 6 months) and monthly

thereafter under Telazol anesthesia (initial loading dose 2–4 mg/kg i.v., then maintained with 0.4 mg/kg per hour). With the animal in a supine position, an endoscope with an attached Sony CCD (Sony Corp., Tokyo, Japan) video camera was inserted to visualize and record vocal fold motion at the level of the glottis. Spontaneous motion induced by hypercapnia was recorded, digitized, and saved on a hard disk for off-line analysis. Because the magnification of each image varied with endoscopic position, a 3-mm ruler was placed on the vocal fold for calibration. Selected still frame images indicative of the passive and hypercapnic airway were analyzed with computer software (Photoshop CS6, Adobe System Inc, San Jose, CA). The numbers of pixels within the circumscribed whole glottal areas were counted for each image. To compensate for size differences in the larynges across animals, we used the value of a normalized glottic area (NGA). This was defined as the measured glottal area divided by the square of the distance between the anterior and posterior commissures of the non-stimulated larynx, and expressed as a percent (*100%). In the four animals implanted with an EMG system, electrophysiologic data was also obtained during these endoscopic sessions.

CO_2 administration trial

To assess any return of vocal fold motion with reinnervation in an anesthetized animal, carbon dioxide mixed with room air was administered to boost respiration toward that which might occur in the awake, exercising animal. A plethysmographic belt transducer was positioned around the chest wall to monitor recordings of chest wall expansion with respiration on an oscilloscope. The oscilloscope trace was monitored by video and the image was superimposed on the endoscope CCD image using a digital AV mixer. The split-screen television imaging allowed inspiratory and expiratory chest movements to be compared with spontaneous opening or closing of the glottis. Carbon dioxide mixed with room air was administered orally at a rate of 5 L/min for 60 seconds. The split-screen video recordings were taken during the CO_2 delivery and for an additional 120 seconds to allow full return to baseline respiration. For computer measurement and analysis of whole glottal area, digitized still frame images were obtained every 10 seconds at peak

inspiration and peak expiration. The results from preoperative CO_2 trials were used for normal data.

Treadmill test

Before implant surgery, each canine was acclimated to run on the treadmill over the course of eight trials during baseline data collection. A sensor was placed on the tail to measure blood hemoglobin oxygen saturation and heart rate with a pulse oximeter (Ultra cap N- 6000, Nellcor Puritan Bennett, LLC, Pleasanton, CA). The tail was carefully shaved the day before each treadmill test to enhance detection of the sensor infrared signal. A relatively strenuous exercise protocol was adopted to distinguish animals with normal exercise tolerance from those that were deficient. The full treadmill test comprised a 12-minute course of 3-minute runs at four levels of sequentially increasing speed (4, 5.3, 6.7, and 8 mph). If the hemoglobin oxygen saturation level dropped below 90% or the animal developed stridor at any time over the course, the treadmill was stopped and the exercise time recorded to obtain the endpoint of tolerance. Animals were tested with the stimulator off.

Electromyography

In the terminal session on seven animals, a midline incision was made and both SLNs and thyroid alae exposed in the anesthetized animal. Nerve stimulation cuffs were placed on the internal branch of the SLNs to evoke RGC responses from the PCA and TA muscles. A thyroplasty window was made on each side and hook wire EMG electrodes inserted into each TA muscle. The DBS electrodes were detached from the IPG and interfaced with a preamplifier to record EMG responses from the PCA muscles. EMG responses were rectified and integrated during stimulation of one of the SLNs and displayed on an oscilloscope. The value obtained for each muscle reflected the magnitude of each EMG response. In the four animals implanted with chronic EMG systems, the responses evoked

in the final five sessions were averaged to obtain an index of final reinnervation status of the PCA and TA muscles.

Statistics

All longitudinal data (passive and dynamic airway, exercise tolerance, EMG) were analyzed using a growth curve modeling method [51] to find out if the group effect for each outcome measure was significant. This analysis method, implemented in the R mixed effect modeling function *lmer* [52], treated the time as a continuous variable and provided a way to handle missing data at some time points. In this growth curve model, the factor of experimental groups, which represented different stimulus frequencies, was treated as a fixed effect. Individual growth function was treated as a random effect, which indicated the growth curve for each canine in a group varied randomly from the average growth curve of that group with a mean difference of zero. Growth curve modeling was performed with second- or third-order polynomial functions. The model parameters indicated whether the groups differed in initial post-intervention baseline value, in end-point asymptotic value and in the average value throughout the study period. Statistical significance (p-value) for individual parameter estimates was assessed using the normal approximation. The level of significance was set at 0.05. If a significance was obtained for the group effect, pairwise comparisons were further performed. A two-way analysis of variance (ANOVA) with repeated measures was performed to test if the differences in preoperative passive and dynamic airway among 4 groups were significant. For the terminal EMG data, a non-parametric Kruskal-Wallis test was performed to test whether the data had the same distribution across groups. All statistical analyses were performed using RStudio [Version 0.99.902. RStudio Team (2015). RStudio: Integrated Development for R. RStudio, Inc., Boston, MA http://www.rstudio.com/], which is a full-featured, user-friendly, integrated development environment for R [Version 3.3.0, R Core Team (2016). R: A language and environment for statistical computing. R Foundation for Statistical Computing, Vienna, Austria. https://www.R-project.org/].

To allow for better growth curve modeling, all longitudinal data were analyzed in the form of post-operative monthly time bins. Specifically, the data obtained between day 0 and day 15 were collapsed and averaged for Month 0 for each individual animal; those obtained from day 16 to day 45 were for Month 1, and so on. The data obtained after day 225 were highly asymptotic and therefore collapsed for Month 8 and beyond (Month 8). The selection of time bin at a monthly interval was based on the consideration of obtaining a trade-off balance between statistical power, which required more data and therefore a larger time window, and temporal resolution, which required a smaller time window but decreased the statistical power. In addition, the scientific rationale that the RLN regenerated relatively slow in canines and the outcome measures only varied minimally within a monthly time window has lent strong support to the selection of monthly time bins.

RESULTS

Endoscopy

a. Preoperative findings

Before nerve section, endoscopic measurements of the glottal airway during a 60 second exposure to CO_2 showed a dramatic increase (Figure 8). NGA increased from a passive airway (i.e. area of glottal opening at 0 second) of about 22% to a dynamic airway (i.e. area of glottal opening at 60 seconds) of about 38% due to the recruitment of PCA inspiratory motoneurons in response to hypercapnia. There was no significant difference ($p=0.16$) among the 4 groups, which indicated all the canines started with the same level of passive and dynamic airway preoperatively.

b. Post-operative passive airway

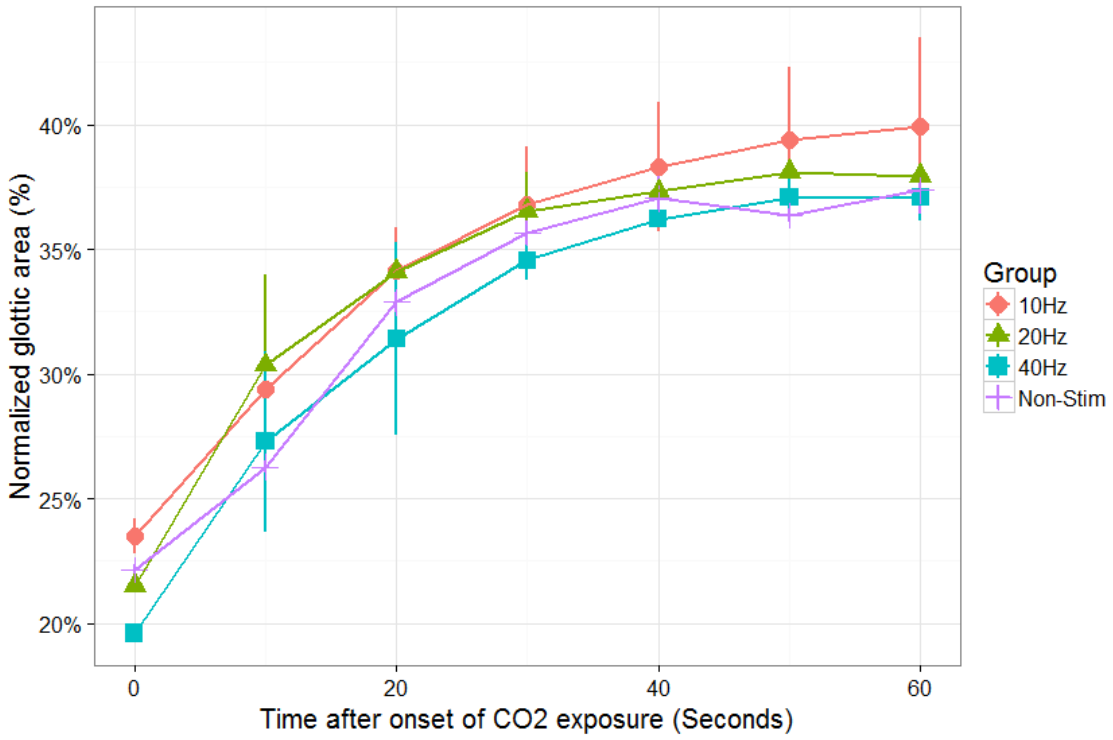

Figure 8. Glottal opening as a function of time following exposure of CO_2 mixed with room air in four groups of animals before RLN transection.

Following nerve transection and anastomosis, there was an immediate decrease in passive airway in all animals due to denervation. As reinnervation took place in abductor and adductor muscles, the passive airway was subject to further change depending on the severity of synkinesis. The passive airway of each experimental group and model curve fits were plotted against post-operative time (Figure 9). There was a significant effect on the average passive airway between the 10Hz group and the rest of the three groups (10Hz vs 20Hz: $p=0.048$, 10Hz vs 40Hz: $p<0.001$, and 10Hz vs Non-stimulated: $p<0.001$). This indicated the 10Hz group had an overall larger passive airway compared to the other three groups throughout the entire study. Further pairwise comparisons did not show any significant difference in the average passive airway among the 20Hz, the 40Hz and the non-stimulated animals. In addition, there was significant difference in the end-point passive airway (i.e. mean passive airway at 8 months and beyond). The end-point passive airway of the 10Hz group was significantly greater than the 40Hz group ($p<0.001$) and the non-stimulated group ($p<0.001$), but not significantly different from

the 20Hz group (p=0.08). Again, no significant difference in the end-point passive airway was obtained among the 20Hz, the 40Hz and the non-stimulated group. Interestingly, the 10Hz animals also had significantly greater baseline passive airway at Month 0 than the 40Hz (p<0.001) and the non-stimulated group (p<0.001).

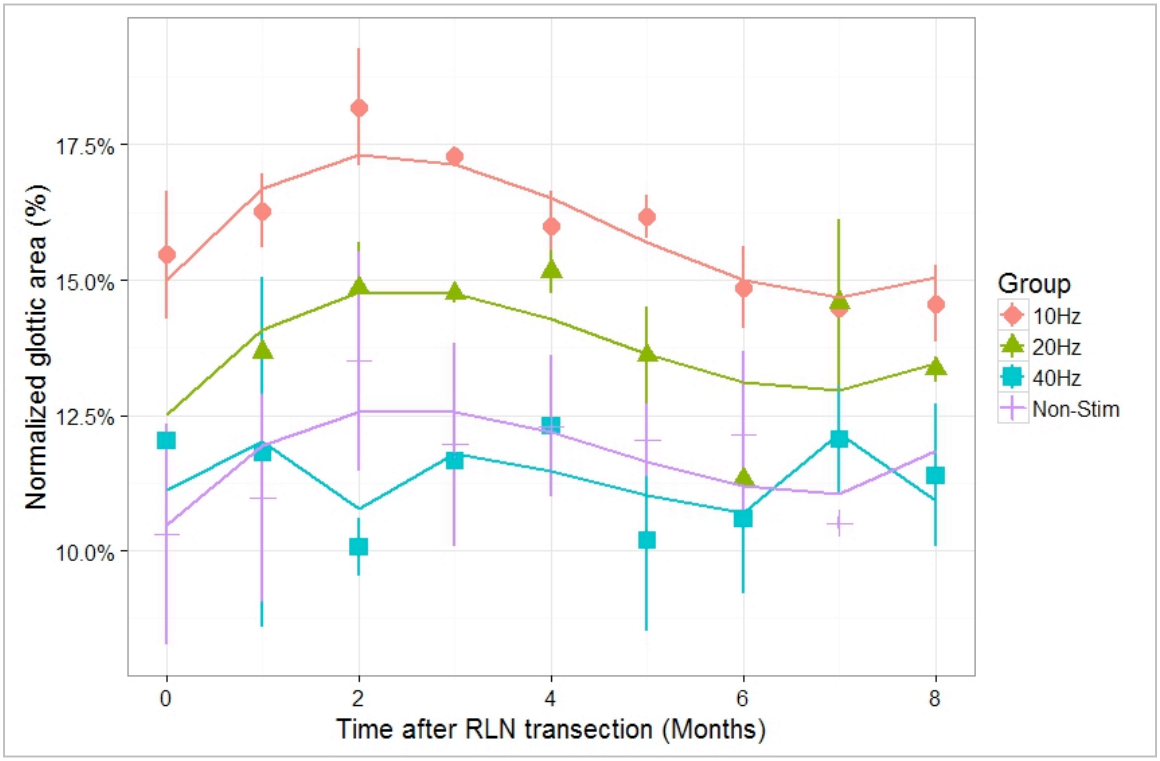

Figure 9. The passive airway and model curve fit for each group following RLN section and anastomoses. All the symbols and corresponding error bars represent the means and standard errors, respectively. A third-order polynomial was applied for growth curve modeling.

c. Post-operative dynamic airway

The dynamic airway of each experimental group and model curve fits were plotted in Figure 10. Similar to the findings in passive airway, the average dynamic airway of the 10Hz group was significantly greater compared to the 20Hz (p=0.001), the 40Hz (p<0.001) and the non-stimulated group (p<0.001). The latter three groups did not have significantly different average dynamic airway compared to each other. In addition, the 10Hz group had a significantly greater end-point dynamic airway than the 20Hz

(p=0.006), the 40Hz (p<0.001) and the non-stimulated group (p<0.001). No significant difference in the end-point dynamic airway was obtained among the latter three groups. The 10Hz group also differed in the baseline dynamic airway at Month 0 compared to the other three groups.

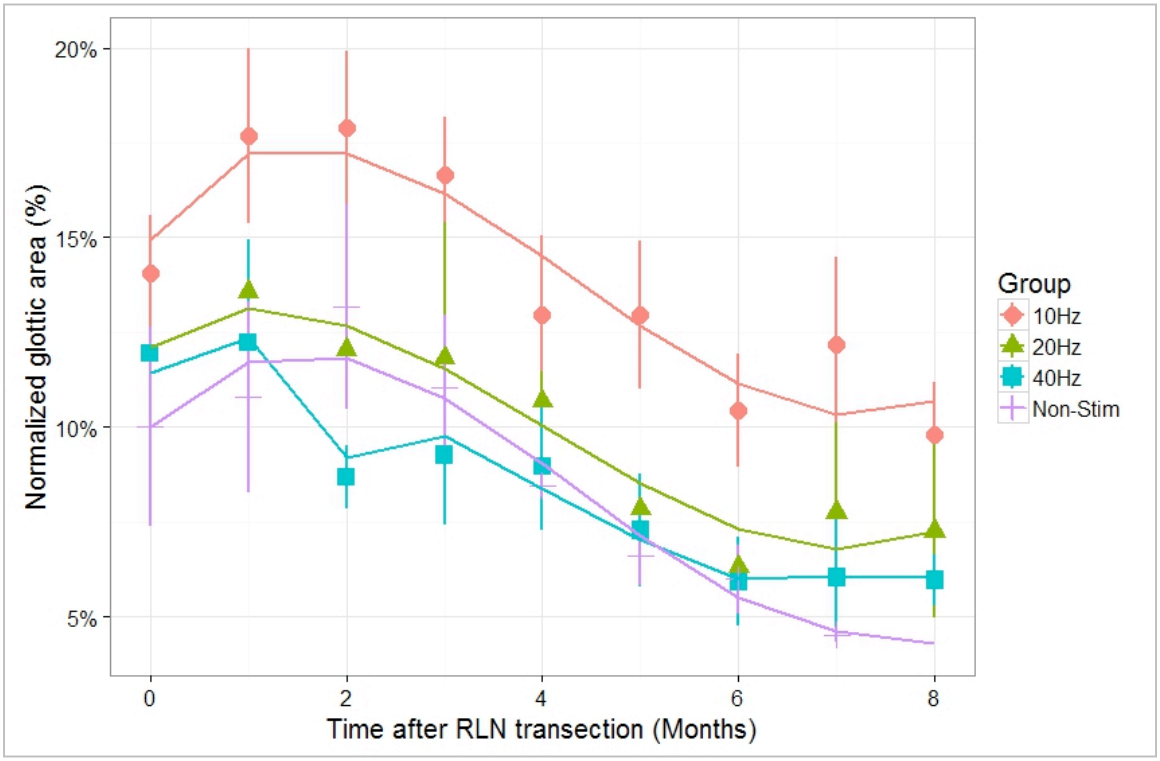

Figure 10. The dynamic airway and model fit for each group following RLN section and anastomoses. The data were shown in the form of mean (symbols) and standard errors (error bars). A third-order polynomial was applied for growth curve modeling.

d. The active component of the glottal airway change

As synkinetic reinnervation of the TA muscle and other adductors occurred by inspiratory motoneurons, a dynamic decrease in the airway occurred with CO_2 administration in all groups. The magnitude of the dynamic airway could reflect the level of synkinetic reinnervation of the adductor muscles by inspiratory motoneurons. However, although these groups differed in the level of their dynamic airways, they also

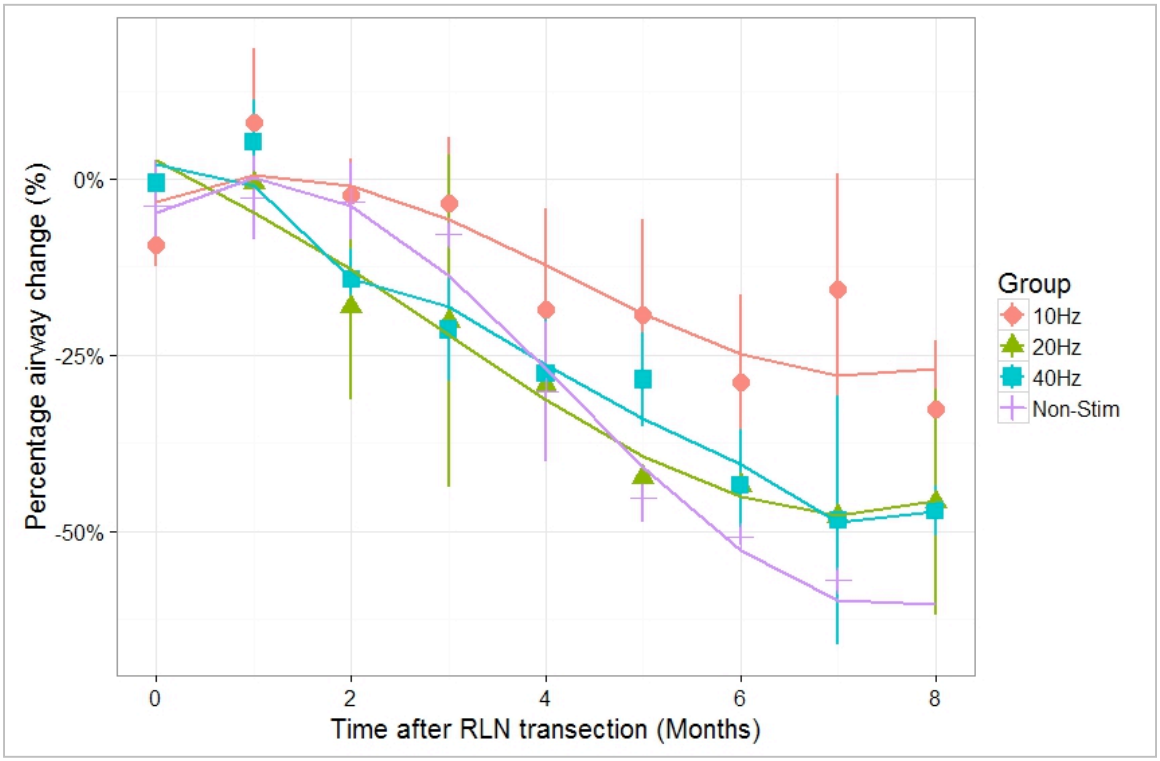

Figure 11. The percentage change of dynamic airway in relative to the passive airway over time [i.e. Percentage change = (Dynamic airway - Passive Airway)/Passive Airway * 100%].

differed in their passive airways. Thus, one could argue that the differences in dynamic airways may have simply reflected the differences in their starting passive airways. For this reason, an estimate of the active component of glottal closure due to synkinetic inspiratory drive was developed. The passive NGA component was subtracted from the dynamic NGA component and expressed as a percent of the passive NGA. This percentage reflected the airway change relative to the starting passive airway. It gave an index of the relative forces generated by the inspiratory motoneurons in the adductor muscles versus the abductor muscle. The results are shown in Figure 11. Specifically, a positive change indicated active enlargement of the airway by administration of CO_2, while a negative change indicated the level of active closure of the airway. It can be noted that there was an active closure in all groups. The average percentage airway closure of the 10Hz group over the entire study was significantly smaller than the non-stimulated group ($p=0.03$), but it was marginally different from the 20Hz ($p=0.05$) and the 40Hz group ($p=0.07$). However, as the majority of synkinetic reinnervation actually

occurred after 3 months, a more appropriate indication of the level of synkinesis was the end-point percentage airway change. At greater than 8 months when the synkinesis became stabilized and the airway change reached an asymptote, the 10Hz group demonstrated significantly smaller percentage airway change than the 20Hz ($p=0.04$), the 40Hz ($p=0.04$) and the non-stimulated group ($p=0.004$). These results indicated that the 10Hz group not only had a greater passive airway and dynamic airway, but also had less synkinetic inspiratory reinnervation of the adductor muscles compared to the other three groups. It also indicated that the significantly greater dynamic airway in the 10Hz group was not simply a reflection of its greater passive airway, but a level of more appropriate reinnervation of the laryngeal muscles. Finally, it can be noted that there was no significant difference in baseline percentage NGA change across all groups of animals at Month 0 before any reinnervation had occurred. The changes in all 4 groups were not different from 0 ($p>0.5$).

These findings were exemplified by individual glottal photos from each animal in Figure 12. Images of the typical glottal airway after the final stage of reinnervation are shown at rest (i.e. passive airway, top frames) and at the end of CO_2 administration (i.e. dynamic airway, bottom frames). All three 10Hz stimulated animals had greater passive and dynamic airways.

Treadmill

Both the graphical and pictorial endoscopy data together suggested that the level of physical activity that an awake animal could tolerate would differ among the study groups. Exercise tolerance was only minimally impaired or not impaired initially

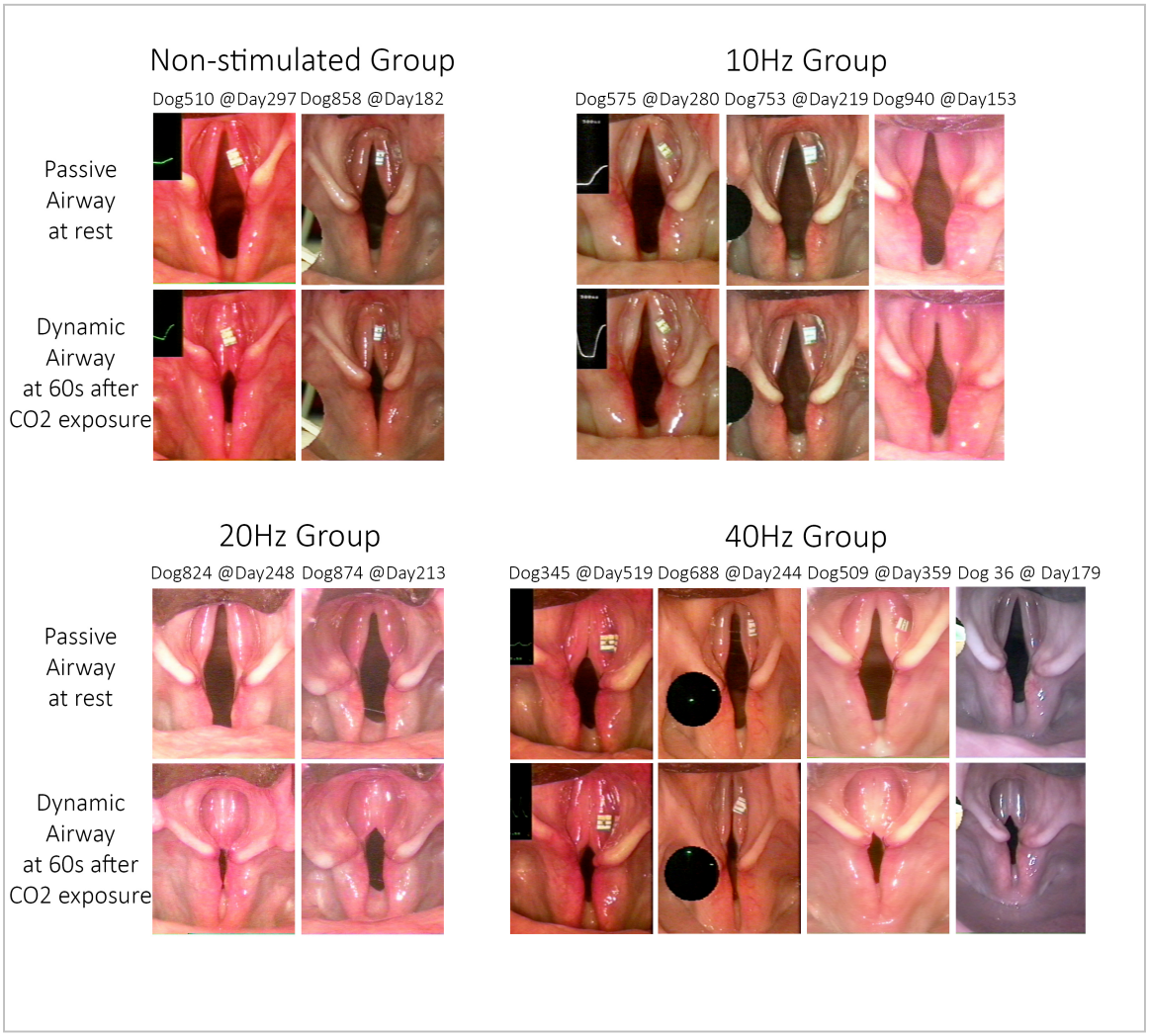

Figure 12. Images of the glottal airway for each animal at rest and following CO_2 administration. All these images represented the glottal openings that reached a stable level after significant reinnervation occurred in each animal. All three 10Hz animals had greater passive and dynamic airways.

following denervation. In the early reinnervation phase, most animals were still able to finish a 12-minute test. After significant reinnervation occurred, the narrowing of the passive airway combined with the tendency for dynamic closure from hypercapnia (or hypoxia) presented as dyspnea and impaired treadmill performance in most animals. In all the 20Hz, 40Hz and non-stimulated control animals, exercise tolerance eventually dropped below 4 minutes while walking at the minimum treadmill speed. Strikingly, only two animals of the 10Hz group were able to run the entire treadmill course for almost all tests throughout the study period for as long as 20 months. The third 10Hz animal (#940)

failed exercise tests beginning at 180 days despite having an adequate dynamic airway. There was a 20 Hz animal (#874) that appeared unhealthy and failed to run greater than 3 minutes at any postoperative test. This animal expired in the cage without any noticeable cause. Autopsy showed epicardial and pulmonary hemorrhage. Undoubtedly, his deficient pulmonary function impaired his treadmill performance, despite a moderate passive airway and dynamic airway upon CO_2 administration. Therefore, the statistical analysis was performed after removing the treadmill data of this animal.

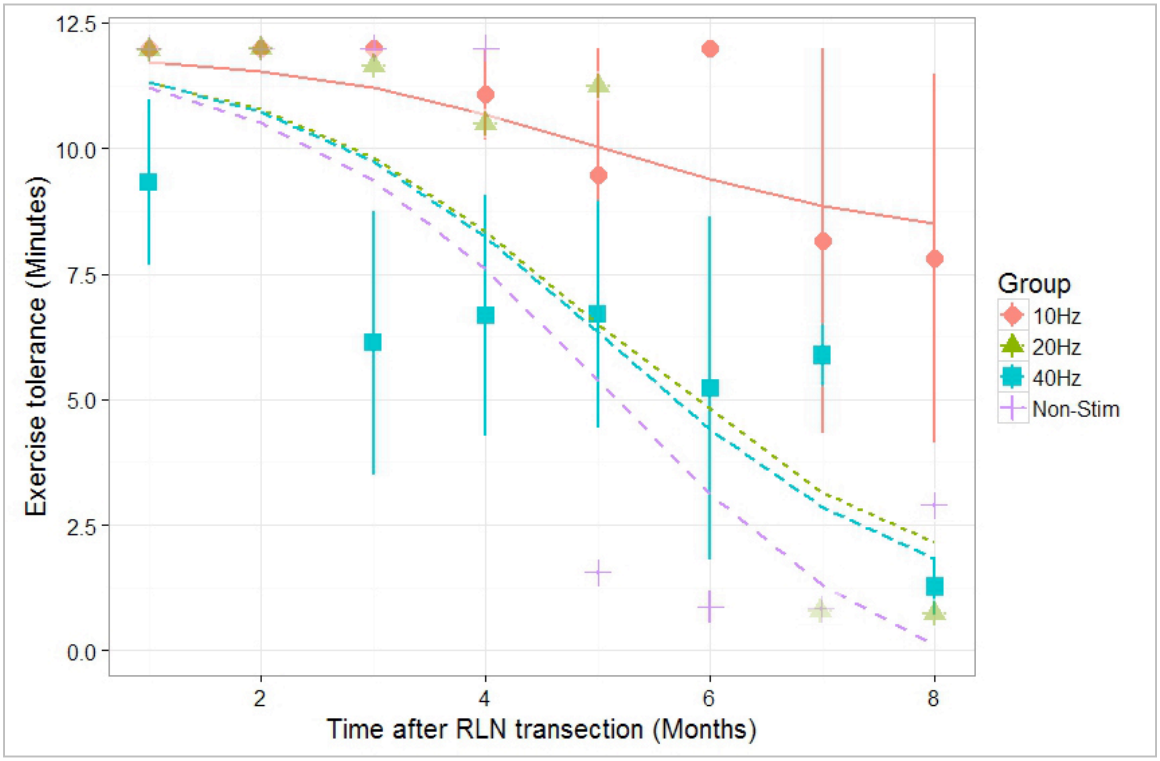

Figure 13. Exercise tolerance evaluated by treadmill performance after RLN transection and model curve fits.

Figure 13 shows the treadmill performance and model curve fits for each group. A logistic function, instead of polynomials, was applied for growth curve modeling for the treadmill data. This was because the non-linear logistic regression is a better way to capture the asymptotic patterns due to the data boundaries that resulted from the nature of the task and measurement (a.k.a. the floor and ceiling effects) [51]. In this case, all treadmill performances were between 0 and 12 minutes because of the experimental

design, not canines' actual physical limit. The 10Hz group had a better end-point asymptotic treadmill tolerance than the 20Hz ($p=0.04$), the 40Hz ($p=0.008$) and the non-stimulated group ($p=0.01$). The latter three groups did not show any significant difference in their treadmill performance at greater than 8 months. Their treadmill performances were consistent with the results from endoscopy.

Electromyography

In the terminal session, rectified/integrated EMG recordings were obtained from the PCA and TA muscles in the anesthetized animal. Recordings were obtained during superior laryngeal nerve stimulation to index reinnervation by RGC motoneurons. A partial set of data was successively obtained, from the three 10Hz animals, both 20Hz animals, one non-stimulated animal, and two 40Hz animals (Table 3). For comparison, evoked response data were also obtained from 6 un-operated control animals with intact nerves. The RGC value was much larger in the TA than PCA muscles in the control animals. Since the PCA muscle in normally innervated animals has no contribution from RGC motor units, the value of 1.22 μVs represented the noise level in the recording. On the other hand, the TA value of 6.84 μVs in control animals reflected the strong innervation of adductor muscles by RGC neurons. All three 10Hz animals had PCA versus TA values that mimicked the un-operated controls, demonstrating little if any foreign RGC reinnervation of the PCA muscles and normal reinnervation of the adductors by these neurons. In stark contrast, the non-stimulated animal showed a complete switch in EMG values between the PCA and TA muscles on both sides. The two 40Hz animals also showed near complete crossover in PCA-TA reinnervation on the both sides. The 20Hz animals both showed a mixed pattern of appropriate reinnervation on one side and inappropriate on the other.

	Normal innervated animals	#575 (10Hz)	#753 (10Hz)	#940 (10Hz)	
Evoked SLN (Intermittent stimulation side)	PCA: 1.218±0.128 TA: 6.839±0.213 **(Mean±SEM, µVs-20ms window, the same below)**	No reliable data	PCA: 3.747±0.264 TA: 8.497±0.235	PCA: 2.516±0.310 TA: 8.033±0.168	
Evoked SLN (Continuous stimulation side)		PCA: 1.225±0.159 TA: 9.289±0.547	PCA: 3.682±0.539 TA: 8.258±0.118	PCA: 2.078±0.395 TA: 10.489±0.486	
	#858 (Non-stim)	**#824 (20Hz)**	**#874 (20Hz)**	**#509 (40Hz)**	**#36 (40Hz)**
Evoked SLN (Intermittent stimulation side)	PCA: 9.543±0.364 TA: 3.894±0.113	PCA: 3.719±0.471 TA: 2.843±0.229	PCA: 2.918±0.146 TA: 5.157±0.411	PCA: 7.205±0.286 TA: 3.841±0.197	PCA: 7.529±0.241 TA: 6.089±0.270
Evoked SLN (Continuous stimulation side)	PCA: 8.315±0.06 TA: 1.452±0.323	PCA: 1.979±0.495 TA: 5.158±0.813	PCA: 3.024±0.322 TA: 1.192±0.217	PCA: 5.748±0.581 TA: 3.419±0.160	PCA: 3.977±0.222 TA: 4.231±0.231

Table 3. Mean RGC recordings from the PCA and TA muscles of the three 10Hz stimulated animals, two 20Hz animals, two 40Hz animals, one non-stimulated animal, and un-operated control animals. Evoked EMG recordings of all the 10Hz animals showed little if any reinnervation of the PCA muscles by foreign RGC motoneurons, similar to the innervated controls. The amount of crossover increased from 10Hz, to 20Hz, to 40Hz, to non-stimulated.

In view of the small sample size, non-parametric statistics were used to analyze the data. To determine the degree of correct reinnervation of the TA muscle, the percentage RGC response in the TA muscle divided by the total response of the TA plus PCA muscles from the same side was calculated. Figure 14A shows the percentage TA response for each group. The data is displayed separately with respect to the muscle conditioning paradigm used (i.e. continuous stimulation versus intermittent stimulation). The conditioning paradigm had no significant effect on outcome ($p=0.81$), indicating that both continuous and intermittent stimulation had the same impact on muscle reinnervation by RGC motoneurons. When the data of both paradigms were pooled together (Figure 14B), the percentage TA response of the 10Hz group was not significantly different from the

un-operated control group, but was significantly greater than all other experimental groups ($p<0.001$).

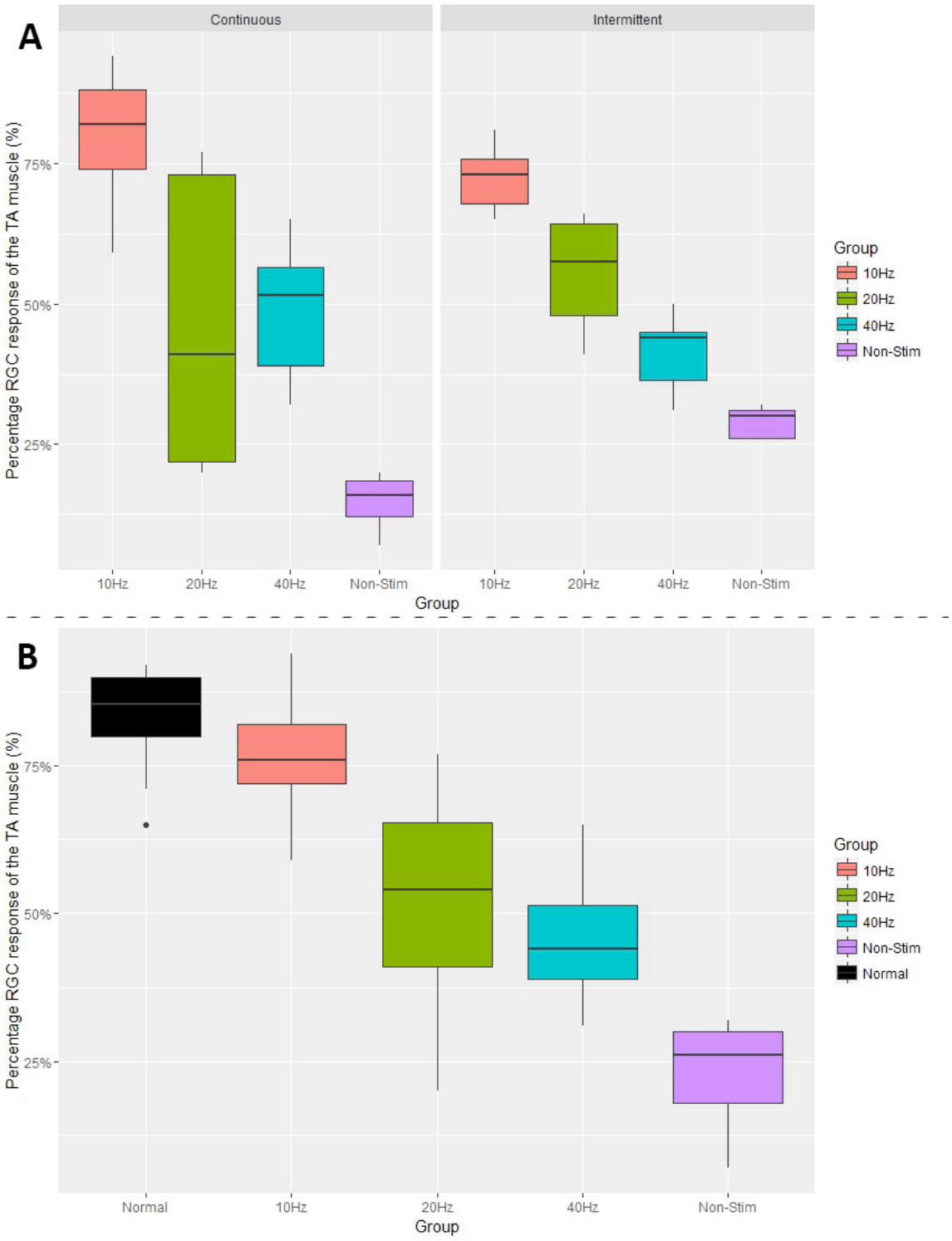

Figure 14. **A** (Top): The percentage RGC response recorded in the TA muscle for each group, shown separately in two stimulus paradigms. Specifically, TA% = TA amplitude / (TA amplitude + PCA amplitude). The higher the TA percentage response indicated the more correct reinnervation by RGC motoneurons. Continuous stimulation did not differ from intermittent stimulation in terms of appropriateness of RGC reinnervation. **B** (Bottom): The 10Hz animals showed the same percentage of TA response as the un-operated, normally-innervated animals, and significantly higher percentage of TA response compared to the other three groups.

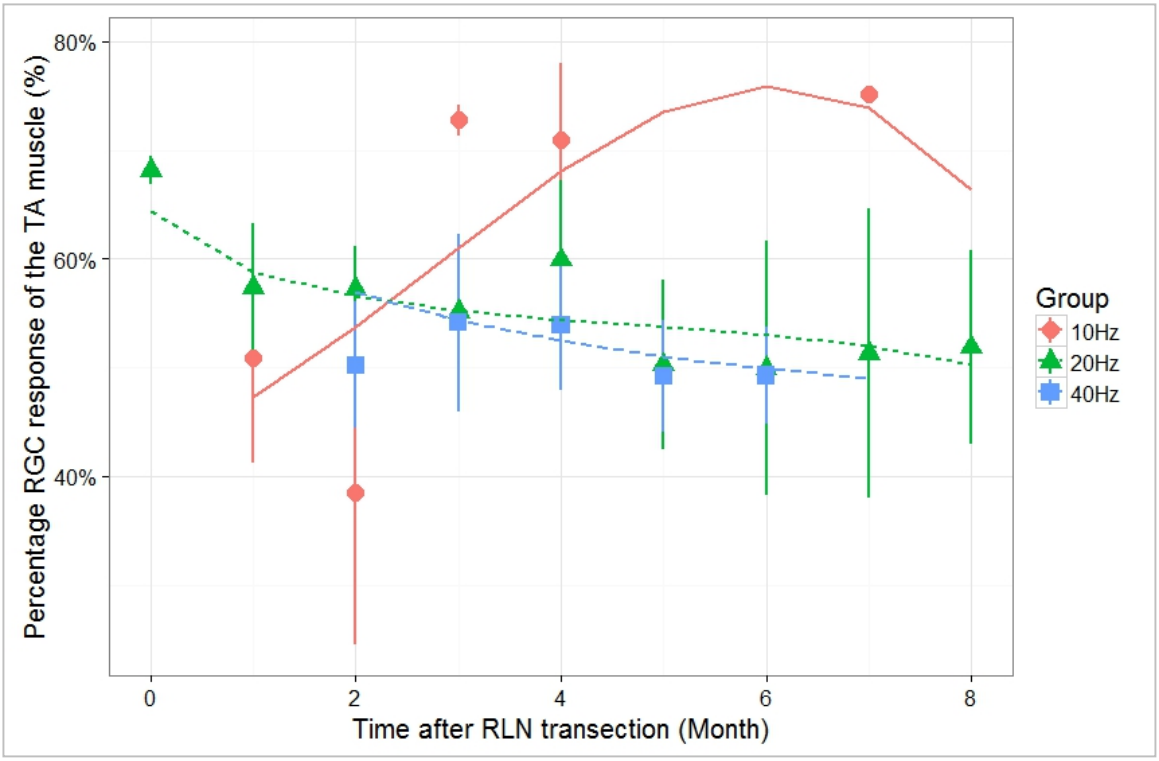

Figure 15. The chronological percentage RGC response recorded in the TA muscle in 4 animals, including one 10Hz, two 20Hz and one 40Hz animals. As reinnervation occurred after RLN transection and became stabilized by 8 months', the 10Hz animals had greater asymptotic percentage of TA response than the 20Hz and 40Hz animals.

In addition to recording in the terminal session, chronological RGC data were also successfully obtained in 4 long-term animals using the implantable EMG recording system that was described in Chapter 1. There were two 20Hz, one 10Hz and one 40Hz animals. Figure 15 shows the percentage TA responses and model curve fits by group. In animals with intact RLN (i.e. un-operated control and pre-nerve-transection animals), RGC responses were exclusively recorded in the TA muscle, and the amplitude of PCA

muscle was at noise level. Therefore, the percentage of TA response was typically between 80%-90% before nerve transection. As reinnervation occurred following RLN transection, a significantly greater level of appropriate RGC reinnervation of the TA muscle was seen in the 10Hz animal. The 10Hz animal had a greater percentage of TA response at greater than 8 months than the 20Hz ($p<0.001$) animals and the 40Hz animal ($p=0.005$). The end-point TA response in the 20Hz animals did not differ significantly from the 40Hz animal ($p=0.87$).

Figure 16 shows an example of the rectified RGC response recorded with SLN stimulation in an un-operated normally innervated animal, a 10Hz, a 20Hz, a 40Hz and a non-stimulated animal. In the un-operated control TA muscle, the RGC response (filled circle) appeared approximately 30ms following the stimulus artifact (vertical spike). As expected, there was no RGC response recorded from the normal PCA (open circle). Only the 10Hz group showed a normal pattern of low PCA and high TA reinnervation by RGC motoneurons. At higher frequencies and non-stimulation, the relative RGC responses between the two muscles changed. In fact, the non-stimulated animal showed complete crossover of the RGC reinnervation of the PCA muscle.

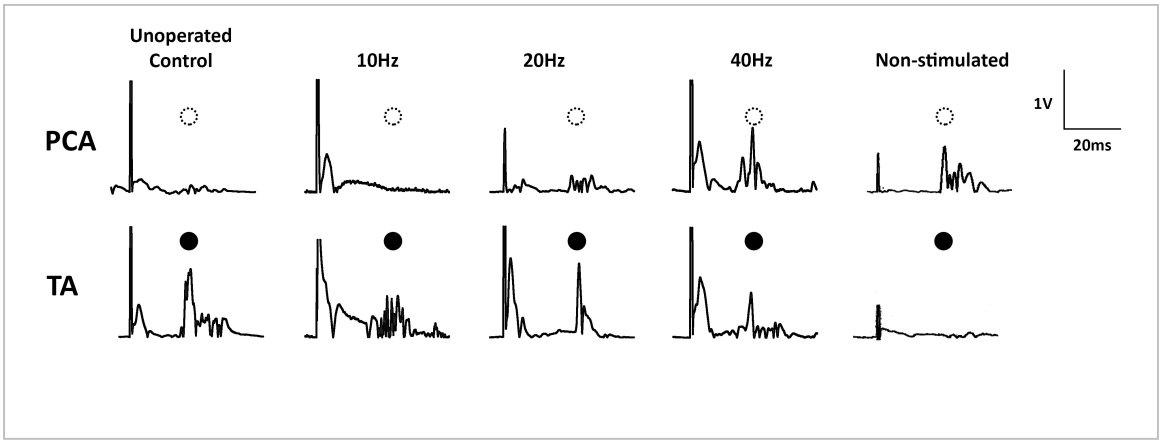

Figure 16. Example of rectified RGC recordings obtained from all five groups of animals in Table 3.

DISCUSSION

Overall, these data suggested electrical stimulation of the denervated PCA muscle with a low frequency, which is characteristic of the intrinsic activity of the PCA muscle, promoted selective reinnervation by its original inspiratory motoneurons. The significant difference obtained between the 10Hz group and the other three groups across all outcome measures consolidates the reliability of the results despite the small sample size in this study.

The glottal airway measured by endoscopy was a direct reflection of the balance of forces generated by abductor versus adductor muscles across the arytenoid joint. The passive airway was an indication of such balance of forces when the animal breathed at a normal rate, during which only a small amount of inspiratory motoneurons were active. When the inspiratory drive was boosted up by hypercapnia, additional inspiratory motoneurons were recruited until the maximal inspiratory effort was reached. As synkinetic reinnervation occurred in all animals, the difference in their passive airway or dynamic airway may partially indicate the degree of appropriate versus aberrant reinnervation by inspiratory motoneurons. However, such difference may also have reflected the individual variation in the anatomical structure of the glottis, as demonstrated by the baseline difference in their passive airways and dynamic airways at Month 0, when no reinnervation could have occurred at such early stage of the study based on previous findings in our laboratory. The variation in glottal anatomy may include size, vertical angle and anterior-posterior asymmetry of the vocal folds. Use of normalized glottal area could offset some variation, such as the difference in size of glottis and endoscope magnification. However, it is unclear to what extent the vertical angel and anterior-posterior asymmetry may have impacted the measure of the glottal opening. As a matter of fact, the preoperative endoscopic measure (Figure 8) did not show any significant time*group interaction on the normalized glottal area, indicating that these factors affected both the passive airway and the dynamic airway to the same extent. Therefore, use of active component (i.e. percentage change in NGA) provided a strategy to cancel

out any variation in anatomical structure between animals. Thus it gave an accurate index of the level of appropriate reinnervation by inspiratory motoneurons. As reinnervation occurred in both the PCA and the TA muscles, the 10Hz animals demonstrated not only greater passive airway and dynamic airway, but more importantly, smaller percentage of synkinetic glottal closure than the other three groups of animals in asymptotic levels. Altogether, these results suggested electrical stimulation of the denervated PCA muscle with low frequency enhanced reinnervation of the muscle by its original inspiratory motoneurons and inhibited subsequent synkinetic reinnervation of the TA muscle by the inspiratory motoneurons.

Use of the active component also addressed the concern of any difference in glottal opening due to incomplete nerve injury. As shown in Figure 11, there was no baseline difference in the percentage airway change at Month 0, and all animals had zero percent airway change. Therefore, it indicated that no vocal fold abduction or adduction was observed immediately after RLN transection. Denervation in all animals was complete.

Notably, in the early reinnervation period (< 2 months), the growth curve model demonstrated a small increase in both the passive airway and the dynamic airway in all groups of animals. The increase in dynamic airway presumably reflected the PCA muscle reinnervation by inspiratory motoneurons, before these motoneurons reached the TA muscle. The increase in passive airway, on the other hand, could have reflected the PCA muscle hypertrophy due to electrical stimulation combined with TA muscle atrophy. Alternatively, it may have reflected early PCA muscle reinnervation by tonically active motoneurons. As significant reinnervation occurred in both the PCA and the TA muscles, synkinesis was present in all animals, starting from approximately three months after RLN injury. All endoscopic measures had reached asymptotes by approximately 7 months. Therefore, the critical period of reinnervation was between 2 and 7 months after RLN injury. In this sense, any intervention taken to prevent synkinesis and to promote selective reinnervation should be performed mainly during this period of time.

The endoscopic findings correlated well with the treadmill performances. Overall, the 10Hz group had a better exercise tolerance than the other three groups. Compared to the endoscopic measure of glottal opening, which was a reliable indicator of ventilatory function as well as muscle reinnervation, the results of treadmill performance were subject to the impact from some other factors, such as the animal's physical condition. For instance, one of the 20Hz canines (#874) failed all treadmill tests except one despite an adequate dynamic airway shown by endoscopy. His final autopsy report showed severely impaired cardiac and pulmonary function, which justified removal of his data from statistical analysis. In addition, unlike the case of endoscopy data, the growth curve analysis with polynomials may not be appropriate in fitting the treadmill data, which had a boundary due to the nature of the assessment [51]. Therefore, proper analysis should be carefully chosen for these data.

Results of both endoscopy and treadmill provided good estimates of the correct versus incorrect reinnervation by inspiratory motoneurons. EMG responses by stimulation of SLN, on the other hand, showed the correct versus incorrect reinnervation by RGC motoneurons. Again, the 10Hz group displayed a normal pattern of RGC reinnervation, which was comparable to the un-operated control. They also significantly differed from the other three groups, which showed differing degrees of aberrant reinnervation of the PCA muscle by RGC motoneurons. The findings in terminal EMG sessions correlated well with the chronological RGC recordings from 4 animals. Therefore, the 10Hz group not only had more appropriate reinnervation of the PCA muscle by the inspiratory motoneurons, but also had more appropriate reinnervation of the TA muscle by the RGC motoneurons. Interestingly, the continuous stimulation did not differ from the intermittent stimulation in terms of inducing proper RGC reinnervation. Although the mechanism is unknown, it suggests that patients may only need to receive the stimulation of the target muscle once or twice a week to promote appropriate reinnervation and to improve functional outcome.

As mentioned in the introduction of this chapter, one underlying hypothesis of this study was that activity dependent muscle plasticity that controls the contractile speed and

histochemistry of a muscle may extend to include the muscle's receptor preference for certain types of motoneurons. These results have proved the prediction that selective reinnervation of the PCA muscle occurred if the imposed activity simulated that of its native inspiratory neurons (10Hz). In addition, if no activity or stimulus activity more characteristic of antagonist RGC motoneurons (40 Hz) was used, the abductor muscle became occupied by foreign RGC motoneurons in abundance. This was not unexpected since RGC motoneurons are four times more plentiful than the inspiratory motoneurons as stated previously. It was difficult to tell if stimulation with a frequency that was more characteristic of antagonist motoneurons (40Hz) would exacerbate the synkinesis compared to no stimulation. All the above findings again support the notion that there was a specific range of activity that maintained a denervated muscle's genetic expression, chemistry, and selective reconnection at the neuromuscular junction in the adult injured nervous system. There was a trend in all outcome measures that the 20Hz group had better, although not significantly, group averages than the 40Hz and the non-stimulated control animals. The non-significance of the 20Hz animal data may have reflected the small sample size. If our hypothesis is right, it would be expected that the 20Hz animals would show significantly better outcome measures than the 40Hz and non-stimulated animals. Similarly, significantly different outcome measures between the 40Hz and the non-stimulated group would be expected with a larger sample size.

The mechanism of selective reinnervation at a molecular and genetic level is yet to be investigated. A possible explanation is that activity-dependent genetic expression influences the affinity of muscle endplates for particular regenerating motoneurons. Muscle stimulation could increase the release of neurotrophic factors, which then promote regeneration of inspiratory motoneurons down the endoneurial tubes at the anastomotic site [9]. Another possibility is that activation with a frequency intrinsic to the muscle prevents the formation of extrajunctional receptors that are non-selective with respect to reconnecting motoneurons.

In the future, ES could be applied to improve muscle integrity and voluntary function by inducing physiologic or genetic changes that are retained after the stimulation is

discontinued. In case of laryngeal paralysis, irrespective of unilateral type or bilateral type, the natural laryngeal functions (i.e. voicing, breathing, and swallowing) could be restored through neuromuscular modulation of the abductor and/or adductor muscles, so that further long-term intervention may not even be necessary. Stimulation applied during a critical period of regeneration may lead to a postsynaptic platform that is receptive to the original motoneurons and regain appropriate neuromuscular connections. In essence, the goal would be to cure rather than to treat paralysis [9].

CONCLUSION

Electrical stimulation of the denervated PCA muscle with a low frequency, characteristic of the intrinsic activity of PCA inspiratory motoneurons, inhibited synkinetic reinnervation by RGC motoneurons, promoted selective reinnervation by its original inspiratory motoneurons, and improved functional recovery.

REFERENCES

1. Zealear, D.L. and C.R. Billante, *Neurophysiology of vocal fold paralysis.* Otolaryngol Clin North Am, 2004. **37**(1): p. 1-23, v.

2. Zealear, D.L., et al., *Electrical stimulation of a denervated muscle promotes selective reinnervation by native over foreign motoneurons.* J Neurophysiol, 2002. **87**(4): p. 2195-9.

3. Insalaco, G., et al., *Thyroarytenoid muscle activity during hypoxia, hypercapnia, and voluntary hyperventilation in humans.* J Appl Physiol (1985), 1990. **69**(1): p. 268-73.

4. Ludlow, C.L., F. Van Pelt, and J. Koda, *Characteristics of late responses to superior laryngeal nerve stimulation in humans.* Ann Otol Rhinol Laryngol, 1992. **101**(2 Pt 1): p. 127-34.

5. Mueller, A.H., *Laryngeal pacing for bilateral vocal fold immobility.* Curr Opin Otolaryngol Head Neck Surg, 2011. **19**(6): p. 439-43.

6. Li, Y., et al., *Comparison of ventilation and voice outcomes between unilateral laryngeal pacing and unilateral cordotomy for the treatment of bilateral vocal fold paralysis.* ORL J Otorhinolaryngol Relat Spec, 2013. **75**(2): p. 68-73.

7. Hydman, J. and P. Mattsson, *Collateral reinnervation by the superior laryngeal nerve after recurrent laryngeal nerve injury.* Muscle Nerve, 2008. **38**(4): p. 1280-9.

8. Crumley, R.L., *Laryngeal synkinesis revisited.* Ann Otol Rhinol Laryngol, 2000. **109**(4): p. 365-71.

9. Zealear, D.L., et al., *Stimulation of denervated muscle promotes selective reinnervation, prevents synkinesis, and restores function.* Laryngoscope, 2013.

10. Connor, N.P., et al., *Tongue muscle plasticity following hypoglossal nerve stimulation in aged rats.* Muscle Nerve, 2013. **47**(2): p. 230-40.

11. Misono, S. and A.L. Merati, *Evidence-based practice: evaluation and management of unilateral vocal fold paralysis.* Otolaryngol Clin North Am, 2012. **45**(5): p. 1083-108.

12. Benjamin, B., *Vocal cord paralysis, synkinesis and vocal fold motion impairment.* ANZ J Surg, 2003. **73**(10): p. 784-6.

13. Crumley, R.L., *Unilateral recurrent laryngeal nerve paralysis.* J Voice, 1994. **8**(1): p. 79-83.

14. Horsley, J.S., *Suture of the Recurrent Laryngeal Nerve.* Ann Surg, 1910. **52**(2): p. 287-8.

15. Crumley, R.L., *Phrenic nerve graft for bilateral vocal cord paralysis.* Laryngoscope, 1983. **93**(4): p. 425-8.

16. Tucker, H.M., *Human laryngeal reinnervation: long-term experience with the nerve-muscle pedicle technique.* Laryngoscope, 1978. **88**(4): p. 598-604.

17. Tucker, H.M., *Human Laryngeal Reinnervation.* Laryngoscope, 1976. **86**(6): p. 769-779.

18. Miehlke, A., *Rehabilitation of Vocal Cord Paralysis - Studies Using Vagus Recurrent Bypass Anastomosis, Type Ramus Posterior Shunt.* Archives of Otolaryngology-Head & Neck Surgery, 1974. **100**(6): p. 431-441.

19. Marina, M.B., J.P. Marie, and M.A. Birchall, *Laryngeal reinnervation for bilateral vocal fold paralysis.* Curr Opin Otolaryngol Head Neck Surg, 2011. **19**(6): p. 434-8.

20. Gordon, T., O.A.R. Sulaiman, and A. Ladak, *Electrical Stimulation for Improving Nerve Regeneration: Where Do We Stand?* Essays on Peripheral Nerve Repair and Regeneration, 2009. **87**: p. 433-444.

21. Zealear, D.L. and C.R. Billante, *Neurophysiology of vocal fold paralysis.* Otolaryngologic Clinics of North America, 2004. **37**(1): p. 1-+.

22. Tamaki, H., et al., *Effect of electrical stimulation-induced muscle force and streptomycin treatment on muscle and trabecular bone mass in early-stage disuse musculoskeletal atrophy.* J Musculoskelet Neuronal Interact, 2015. **15**(3): p. 270-8.

23. Hu, L., et al., *Low-Frequency Electrical Stimulation Attenuates Muscle Atrophy in CKD-A Potential Treatment Strategy.* Journal of the American Society of Nephrology, 2015. **26**(3): p. 626-635.

24. Willand, M.P., et al., *Sensory Nerve Cross-Anastomosis and Electrical Muscle Stimulation Synergistically Enhance Functional Recovery of Chronically Denervated Muscle.* Plastic and Reconstructive Surgery, 2014. **134**(5): p. 736E-745E.

25. Williams, H.B., *The value of continuous electrical muscle stimulation using a completely implantable system in the preservation of muscle function following motor nerve injury and repair: an experimental study.* Microsurgery, 1996. **17**(11): p. 589-96.

26. Cheetham, J., et al., *Effects of Functional Electrical Stimulation on Denervated Laryngeal Muscle in a Large Animal Model.* Artificial Organs, 2015. **39**(10): p. 876-885.

27. Zealear, D.L., et al., *The effects of chronic electrical stimulation on laryngeal muscle physiology and histochemistry.* ORL J Otorhinolaryngol Relat Spec, 2000. **62**(2): p. 81-6.

28. Gharib, N.M.M., et al., *Efficacy of electrical stimulation as an adjunct to repetitive task practice therapy on skilled hand performance in hemiparetic stroke patients: a randomized controlled trial.* Clinical Rehabilitation, 2015. **29**(4): p. 355-364.

29. Fujita, N., S. Murakami, and H. Fujino, *The Combined Effect of Electrical Stimulation and High-Load Isometric Contraction on Protein Degradation Pathways in Muscle Atrophy Induced by Hindlimb Unloading.* Journal of Biomedicine and Biotechnology, 2011.

30. Hoffman, H., *Acceleration and retardation of the process of axon-sprouting in partially devervated muscles.* Aust J Exp Biol Med Sci, 1952. **30**(6): p. 541-66.

31. Skouras, E., et al., *Stimulation of Trigeminal Afferents Improves Motor Recovery After Facial Nerve Injury Functional, Electrophysiological and Morphological Proofs Introduction.* Stimulation of Trigeminal Afferents Improves Motor Recovery after Facial Nerve Injury: Functional, Electrophysiological and Morphological Proofs, 2013. **213**: p. 1-+.

32. Nix, W.A. and H.C. Hopf, *Electrical-Stimulation of Regenerating Nerve and Its Effect on Motor Recovery.* Brain Research, 1983. **272**(1): p. 21-25.

33. Pockett, S. and R.M. Gavin, *Acceleration of Peripheral-Nerve Regeneration after Crush Injury in Rat.* Neuroscience Letters, 1985. **59**(2): p. 221-224.

34. Al-Majed, A.A., T.M. Brushart, and T. Gordon, *Electrical stimulation accelerates and increases expression of BDNF and trkB mRNA in regenerating rat femoral motoneurons.* Eur J Neurosci, 2000. **12**(12): p. 4381-90.

35. Al-Majed, A.A., S.L. Tam, and T. Gordon, *Electrical stimulation accelerates and enhances expression of regeneration-associated genes in regenerating rat femoral motoneurons.* Cellular and Molecular Neurobiology, 2004. **24**(3): p. 379-402.

36. Brushart, T.M., *Preferential reinnervation of motor nerves by regenerating motor axons.* J Neurosci, 1988. **8**(3): p. 1026-31.

37. Al-Majed, A.A., et al., *Brief electrical stimulation promotes the speed and accuracy of motor axonal regeneration.* Journal of Neuroscience, 2000. **20**(7): p. 2602-2608.

38. Doucet, B.M., A. Lam, and L. Griffin, *Neuromuscular electrical stimulation for skeletal muscle function.* Yale J Biol Med, 2012. **85**(2): p. 201-15.

39. Burke, R.E., *Revisiting the notion of 'motor unit types'.* Prog Brain Res, 1999. **123**: p. 167-75.

40. Burke, R.E., et al., *Physiological Types and Histochemical Profiles in Motor Units of Cat Gastrocnemius.* Journal of Physiology-London, 1973. **234**(3): p. 723-&.

41. Burke, R.E., *The structure and function of motor units*, in *Myology : basic and clinical*, A. Engel and C. Franzini-Armstrong, Editors. 2004, McGraw-Hill, Medical Pub. Division: New York. p. 104-118.

42. Buller, A.J., J.C. Eccles, and R.M. Eccles, *Interactions between motoneurones and muscles in respect of the characteristic speeds of their responses.* The Journal of Physiology, 1960. **150**(2): p. 417-439.

43. Bacou, F., et al., *Expression of myosin isoforms in denervated, cross-reinnervated, and electrically stimulated rabbit muscles.* European Journal of Biochemistry, 1996. **236**(2): p. 539-547.

44. Jarvis, J.C., *The Relationship Between Activity Pattern and Muscle Adaptation in Skeletal Muscle.* Artificial Organs, 2015. **39**(10): p. 863-867.

45. Kang, L.H.D. and J.F.Y. Hoh, *Chronic Low-Frequency Stimulation Transforms Cat Masticatory Muscle Fibers into Jaw-Slow Fibers.* Journal of Histochemistry & Cytochemistry, 2011. **59**(9): p. 849-863.

46. Pette, D., *Historical Perspectives: plasticity of mammalian skeletal muscle.* J Appl Physiol (1985), 2001. **90**(3): p. 1119-24.

47. Pette, D. and R.S. Staron, *Mammalian skeletal muscle fiber type transitions.* Int Rev Cytol, 1997. **170**: p. 143-223.

48. Rhee, H.S., C.A. Lucas, and J.F.Y. Hoh, *Fiber types in rat laryngeal muscles and their transformations after denervation and reinnervation.* Journal of Histochemistry & Cytochemistry, 2004. **52**(5): p. 581-590.

49. Zhou, Z., et al., *Reinnervation-induced alterations in rat skeletal muscle.* Neurobiology of Disease, 2006. **23**(3): p. 595-602.

50. Hennig, R. and T. Lomo, *Firing patterns of motor units in normal rats.* Nature, 1985. **314**(6007): p. 164-6.

51. Mirman, D., *Growth curve analysis and visualization using R*. 2014, Boca Raton, FL: CRC Press.

52. Bates D, M.M., Bolker B and Walker S *_lme4: Linear mixed-effects models using Eigen and S4_. R package version 1.1-7*. 2014.